

## Appendix A. Unknown objects observed during out runs at ESO/MPG, Swope and INT.

Table A.1: The asteroids officially discovered at ESO/MPG (according to MPC DISCSTATUS Jan 2011). In the first line we give orbital elements calculated with FIND\_ORB and observational data from our run, while in the second line we include MPC orbital data derived from all available observations.

Acronym	Designation	$a$	$e$	$i$	MOID	$H$	pos	arc	$rms$	$R$	$\beta$	$\epsilon$	$\mu$
VBSO004	2008 EB98	2.94	0.12	7.7	1.58	16.8	18	2d	0.07	20.0	10	176	0.54
		2.90	0.16	7.1		17.2	25	10d					
VBSO008	2008 EF155	2.73	0.05	11.4	1.61	17.3	16	2d	0.14	20.5	11	176	0.60
VBSO036	2008 EG162	2.86	0.21	1.9	1.28	18.5	7	1d	0.24	20.7	2	173	0.54
		2.79	0.18	2.3		18.2	15	23d					
VBSO052	2008 EV168	2.49	0.06	3.3	1.33	17.5	8	1d	0.10	20.1	2	163	0.57
		2.41	0.16	2.7		18.2	16	24d					
VBSO059	2008 EF151	2.36	0.01	7.4	1.33	17.7	8	1d	0.06	20.3	2	163	0.62
		2.33	0.10	7.5		18.1	24	36d					
VBTO002	2008 ED145	2.25	0.14	4.7	0.93	18.7	11	1d	0.18	20.3	-3	161	0.54
		2.60	0.25	5.1		18.5	23	16d					
VBTO005	2008 ED144	3.43	0.21	9.7	1.76	16.3	30	3d	0.09	20.5	-3	162	0.46
		3.22	0.07	10.5		16.3	40	16d					
VBTO008	2008 EC144	2.23	0.17	7.8	0.86	17.4	14	1d	0.37	20.7	-3	162	0.63
		2.23	0.15	8.1		17.7	30	3d					
VBTO011	2008 EY131	2.54	0.21	3.8	1.03	17.7	30	3d	0.12	20.2	-4	162	0.55
		2.42	0.07	4.4		17.4	66	3y					
VBTO012	2008 EB145	3.08	0.22	8.7	1.39	15.8	22	2d	0.26	21.0	-4	162	0.45
VBTO013	2008 EA145	2.79	0.20	5.6	1.22	17.9	14	1d	0.09	20.4	-4	162	0.49
		3.23	0.07	14.6		15.9	26	16d					
VBTO015	2008 EE145	3.12	0.07	9.2	1.92	16.7	22	2d	0.37	20.6	-3	161	0.46
VBTO021	2008 EN145	2.49	0.21	21.6	1.02	16.2	16	2d	0.10	19.9	-3	162	0.64
		2.24	0.17	6.6		17.5	51	8y					
VBTO022	2008 EK145	2.38	0.38	8.3	0.49	16.9	30	3d	0.13	20.4	-3	162	0.59
VBTO023	2008 EH155	4.11	0.48	10.7	1.17	15.3	22	2d	0.13	20.3	-3	162	0.46
		2.99	0.18	11.3		15.6	29	16d					
VBTO024	2008 EJ145	2.25	0.09	3.8	1.05	17.4	30	3d	0.16	20.4	-3	162	0.59
		2.59	0.16	17.0		16.8	72	5y					
VBTO025	2006 WO37	2.31	0.09	4.4	1.11	18.5	16	2d	0.20	20.6	-3	162	0.55
		2.56	0.08	6.9		17.2	53	5y					
VBTO029	2008 EH145	2.99	0.13	11.1	1.60	17.4	16	2d	0.16	20.6	-4	162	0.52
		3.02	0.14	11.1		17.6	24	16d					
VBTO043	2008 EL145	2.47	0.07	6.1	1.29	17.9	16	2d	0.26	20.9	-4	162	0.55
VBTO055	2008 EO145	2.43	0.05	3.0	1.31	17.7	16	2d	0.08	20.4	-3	162	0.53
VBTO063	2008 EP145	2.08	0.02	6.7	1.02	18.3	15	2d	0.17	20.4	-3	162	0.64
		2.29	0.20	6.9		18.4	37	16d					
VBTO011	2008 EA84	2.90	0.41	14.5	0.71	15.2	4	1d	0.05	20.7	-6	192	0.50

Table A.1 (continued) – Asteroids officially discovered at ESO/MPG.

Acronym	Designation	$a$	$e$	$i$	MOID	$H$	pos	arc	$\sigma$	$R$	$\beta$	$\epsilon$	$\mu$
VBTU012	2008 EX154	2.66	0.35	7.0	0.74	15.7	10	2d	0.09	20.6	-6	192	0.53
		2.77	0.06	5.1		16.8	32	10y					
VBTU013	2008 EU154	2.23	0.05	5.2	1.12	19.0	9	2d	0.27	21.0	-6	192	0.62
VBTU014	2008 EY83	2.06	0.16	4.2	0.74	20.4	5	1d	0.31	21.1	-6	192	0.65
VBTU015	2008 EZ83	3.06	0.18	5.2	1.52	17.2	9	2d	0.12	20.2	-6	192	0.50
		3.10	0.08	6.2		17.0	13	14d					
VBTU016	2008 EW154	2.04	0.31	5.0	0.41	17.7	10	2d	0.13	20.9	-6	192	0.70
VBTU017	2008 EV154	2.55	0.02	15.4	1.49	17.9	10	2d	0.21	21.1	-6	192	0.64
VBTU020	2008 EC145	2.14	0.13	1.8	0.87	19.4	6	1d	0.32	20.8	-3	161	0.55
VBTU049	2008 EL154	2.61	0.22	9.6	1.04	19.5	12	1d	0.16	21.2	-4	189	0.65
VBTU052	2008 EE155	2.56	0.23	6.6	0.97	17.0	12	2d	0.18	21.2	-4	189	0.58
		2.67	0.29	5.8		17.3	17	3d					
VBTU054	2008 ED155	3.05	0.15	3.3	1.61	17.9	18	2d	0.30	21.0	-4	189	0.51
VBTU056	2008 EK154	2.99	0.02	3.7	1.93	17.5	14	2d	0.26	21.2	-4	189	0.52
		2.81	0.31	5.4		16.4	22	3d					
VBTU057	2008 EC155	3.06	0.05	9.3	1.93	17.6	15	2d	0.33	21.3	-4	189	0.53
		3.04	0.09	10.3		17.5	13	3d					
VBTU058	2008 EA155	2.60	0.02	7.8	1.56	17.9	22	3d	0.17	21.1	-4	189	0.60
		2.60	0.02	7.9		17.9	22	3d					
VBTU059	2008 EJ154	2.86	0.31	16.9	1.01	16.3	24	3d	0.17	21.0	-4	189	0.54
		2.89	0.08	11.5		17.0	24	3d					
VBTU060	2008 EB155	3.11	0.14	9.4	1.66	16.5	23	3d	0.24	21.3	-4	189	0.49
		3.20	0.05	7.7		17.0	23	3d					
VBTU061	2008 EZ154	2.25	0.09	3.0	1.06	19.3	10	1d	0.13	21.1	-4	189	0.67
VBTU062	2008 EY154	3.03	0.19	8.9	1.46	17.2	15	2d	0.16	20.8	-4	189	0.55
VBTU063	2008 EK155	2.27	0.23	2.8	0.75	17.7	12	1d	0.25	21.2	-4	188	0.65
VBTU064	2008 EJ155	2.20	0.14	4.2	0.89	19.6	12	1d	0.15	20.8	-4	188	0.66
VBTU074	2008 EG155	2.59	0.05	2.4	1.48	18.5	11	2d	0.13	21.4	-4	189	0.57
VBTU089	2008 EL155	2.85	0.04	9.3	1.75	17.9	11	2d	0.21	21.4	-4	189	0.55
		2.86	0.09	8.0		18.3	15	9d					
VBTU090	2008 EA98	2.48	0.10	4.7	1.24	19.1	3	1d	0.10	21.4	-4	189	0.61
VBTU101	2008 EX152	2.53	0.15	15.4	1.16	16.0	14	1d	0.14	20.4	9	135	0.25
		2.62	0.16	14.0		16.4	44	3y					
VBTU104	2008 EH168	2.62	0.16	6.6	1.21	18.1	9	1d	0.29	20.7	-3	161	0.50
		2.02	0.24	2.6		20.4	17	34d					
VBTU107	2008 EF145	2.67	0.03	4.3	1.60	17.5	17	2d	0.30	20.8	-4	161	0.50

Table A.1 (continued) – Asteroids officially discovered at ESO/MPG.

Acronym	Designation	$a$	$e$	$i$	MOID	$H$	pos	arc	$\sigma$	$R$	$\beta$	$\epsilon$	$\mu$
VBTU113	2008 EG144	2.31	0.38	5.1	0.43	16.1	13	1d	0.12	20.4	0	163	0.59
VBTU124	2008 EJ168	2.80	0.04	2.8	1.68	17.0	21	3d	0.27	20.9	-1	163	0.49
		2.39	0.25	1.9		19.2	21	30d					
VBTU128	2008 EH144	3.03	0.61	4.4	0.19	17.3	19	3d	0.14	20.6	0	163	0.59
VBTU199	2008 EL144	1.77	0.16	14.8	0.56	18.5	21	2d	0.17	20.7	1	132	0.46
VBTU202	2008 EK144	2.52	0.03	9.2	1.45	17.1	21	2d	0.21	21.0	0	132	0.18
VBTU203	2008 EN144	1.84	0.05	23.5	0.75	18.4	14	2d	0.26	20.8	0	132	0.65
VBTU204	2008 EM144	2.79	0.18	21.6	1.28	16.0	16	2d	0.23	21.0	0	132	0.27
VBTU207	2008 EW152	2.09	0.17	2.1	0.76	18.2	13	1d	0.14	20.9	0	131	0.13
		2.80	0.01	3.9		16.6	63	8y					
VBTU208	2008 EE157	3.12	0.07	2.9	1.92	16.8	5	1d	0.06	20.4	1	171	0.51
		2.19	0.37	2.4		20.8	13	24d					
VBTU213	2008 EQ144	2.40	0.20	3.8	0.93	18.5	4	1d	0.07	19.7	1	172	0.59
		2.73	0.03	9.1		17.2	11	16d					
VBTU224	2008 EW144	2.34	0.10	5.8	1.12	17.9	5	1d	0.15	20.1	10	162	0.55

Table A.2: Later identification of unknown asteroids observed at ESO/MPG.  
First line represent our data and second line reffers to updated MPC data.

Acronym	Designation	$a$	$e$	$i$	MOID	$H$	pos	arc	$rms$	$R$	$\beta$	$\epsilon$	$\mu$
VB001	2008 FG67	2.52	0.16	6.0	1.11	17.3	8	1d	0.27	20.4	0	124	0.23
		2.68	0.22	7.2		17.5	28	48d					
VB014	2004 RZ319	2.22	0.23	7.4	0.75	16.7	8	1d	0.07	20.0	0	124	0.14
		3.16	0.02	14.2		15.3	77	11y					
VB018	2008 FZ110	2.63	0.12	4.5	1.33	16.6	8	1d	0.08	20.1	0	124	0.13
		2.52	0.10	4.6		17.2	46	9y					
VB024	2009 TG3	2.21	0.05	5.1	1.10	16.8	8	1d	0.07	20.4	-1	124	0.11
		2.62	0.21	7.2		16.5	47	7y					
VB027	2005 MW44	2.58	0.01	6.0	1.55	16.4	7	1d	0.08	20.5	0	123	0.07
		2.35	0.13	6.0		16.9	64	19y					
VB029	2007 AY28	2.68	0.03	2.5	1.59	16.6	6	1d	0.09	20.7	0	124	0.04
		2.76	0.04	2.6		17.0	46	14y					
VB036	2010 VT31	2.76	0.20	13.6	1.22	15.9	7	1d	0.09	21.1	-1	126	0.16
		3.13	0.22	17.2		15.5	41	7y					
VB037	2001 TB234	2.96	0.11	2.3	1.63	15.2	7	1d	0.07	20.3	-1	126	0.09
		5.14	0.06	3.3		13.3	61	8y					
VB039	2005 SA133	3.18	0.08	2.0	1.91	16.2	7	1d	0.08	20.7	-1	126	0.04
		2.80	0.03	1.8		17.0	52	14y					
VB045	2008 JF20	2.67	0.21	13.2	1.11	17.2	7	1d	0.06	20.2	-1	126	0.32
		2.59	0.19	13.7		16.9	46	78d					
VB047	2008 GD44	3.02	0.03	9.9	1.91	15.9	8	1d	0.06	20.5	-1	126	0.14
		3.06	0.04	10.2		16.0	20	43d					
VB057	2005 TB197	2.32	0.12	2.2	1.05	17.1	8	1d	0.18	21.1	-1	126	0.07
		2.64	0.13	2.4		17.5	29	9y					
VBOP008	2008 EF144	3.30	0.10	2.4	1.92	15.3	8	1d	0.11	19.6	-3	162	0.45
		3.20	0.08	2.5		16.2	54	8y					
VBOP013	2008 EM90	2.38	0.12	3.0	1.11	18.3	8	1d	0.06	20.5	-4	162	0.54
		2.53	0.03	3.9		17.6	45	20d					
VBOP017	2008 EB144	2.37	0.35	6.2	0.55	18.7	8	1d	0.13	19.3	-4	161	0.61
		3.14	0.05	27.1		15.8	45	12y					
VBOP023	2008 EJ144	2.49	0.04	0.9	1.39	17.1	8	1d	0.11	20.3	0	163	0.57
		2.40	0.13	0.6		17.7	19	15d					
VBOP024	2008 EL163	2.72	0.05	2.4	1.60	17.3	8	1d	0.13	20.6	0	163	0.53
		2.91	0.14	1.4		17.8	16	42d					
VBSO007	2008 EG168	2.79	0.35	8.1	0.82	14.2	17	2d	0.36	19.2	11	176	0.53
		2.99	0.16	7.3		15.8	24	45d					
VBSO024	2008 DA83	2.88	0.01	2.6	1.84	16.7	7	1d	0.30	20.3	3	173	0.55
		2.97	0.04	1.9		16.9	32	11y					
VBSO063	2008 ER144	2.26	0.27	4.7	0.66	20.0	8	1d	0.11	20.4	11	184	0.50
VBSO066	2008 ES144	2.69	0.25	6.0	1.05	18.9	8	1d	0.18	20.7	11	184	0.56
		3.17	0.07	11.0		16.8	16	23d					
VBSO068	2008 EZ95	2.34	0.18	6.0	0.94	18.8	8	1d	0.08	20.2	11	184	0.62
		2.53	0.11	7.8		17.8	15	8d					
VBTO001	2008 EJ20	2.47	0.16	6.6	1.06	16.1	15	1d	0.23	19.8	-3	161	0.57
		2.44	0.12	6.2		16.6	126	10y					
VBTO028	2008 EE144	2.53	0.08	14.7	1.32	17.6	16	2d	0.10	20.3	-4	162	0.62
		2.56	0.09	15.8		17.4	27	3d					
VBTO052	2008 EJ134	2.78	0.05	4.0	1.63	16.5	8	1d	0.11	20.4	-3	162	0.52
		2.78	0.07	4.0		17.0	44	6y					

Table A.2 (continued) – Later identification of unknown asteroids observed at ESO/MPG.

Acronym	Designation	$a$	$e$	$i$	MOID	$H$	pos	arc	$rms$	$R$	$\beta$	$\epsilon$	$\mu$
VBTU008	2008 CQ149	2.36	0.01	3.2	1.34	18.5	5	1d	0.12	21.1	-5	192	0.63
		3.21	0.21	9.3		16.4	11	30d					
VBTU019	2008 ET69	2.37	0.11	5.8	1.12	19.0	5	1d	0.13	21.0	-6	192	0.63
VBTU023	2008 DU59	2.41	0.27	2.5	0.78	19.1	4	1d	0.08	20.0	-6	192	0.50
		3.18	0.08	4.1		15.7	41	11y					
VBTU025	2008 EW83	2.36	0.25	3.7	0.78	18.5	6	1d	0.05	19.5	-6	193	0.52
		3.13	0.03	11.0		15.4	62	16y					
VBTU028	2008 EX83	2.29	0.08	7.4	1.12	17.6	6	1d	0.09	19.7	-6	192	0.66
		2.38	0.07	9.2		17.1	53	19y					
VBTU044	2008 EO84	2.74	0.07	3.8	1.55	17.3	18	2d	0.23	21.0	-4	189	0.55
		2.74	0.08	3.6		17.6	27	8d					
VBTU047	2008 EP84	3.11	0.06	9.6	1.90	16.2	14	1d	0.10	20.5	-4	188	0.52
VBTU048	2008 EM84	2.39	0.02	4.3	1.34	18.4	18	2d	0.17	20.9	-4	189	0.62
		2.68	0.31	7.2		17.5	51	2y					
VBTU050	2008 EL84	3.09	0.11	3.9	1.76	17.1	14	1d	0.08	20.6	-4	189	0.53
		3.09	0.09	4.8		16.7	43	6y					
VBTU055	2005 SD127	3.26	0.01	5.8	2.21	16.5	18	2d	0.14	20.9	-4	189	0.48
		3.12	0.19	7.6		16.1	89	17y					
VBTU065	2008 EQ84	2.37	0.08	3.5	1.19	18.3	12	1d	0.10	20.5	-4	188	0.64
		2.37	0.08	3.4		18.6	28	9d					
VBTU098	2008 GS74	2.23	0.05	7.9	1.14	17.4	10	1d	0.24	20.8	9	135	0.18
		2.98	0.09	8.9									
VBTU119	2008 EN90	2.27	0.31	6.7	0.59	19.3	13	1d	0.09	20.1	-1	163	0.69
		2.60	0.05	22.3		16.8	34	44d					
VBTU123	2008 EM154	2.78	0.05	3.3	1.64	16.7	13	1d	0.13	20.6	-1	162	0.51
VBTU125	2008 EO90	2.56	0.02	2.1	1.51	17.2	12	1d	0.11	20.5	-1	162	0.54
		2.58	0.25	2.8		16.9	19	17d					
VBTU136	2008 DE69	2.28	0.02	4.5	1.23	17.4	8	1d	0.07	20.0	-4	189	0.66
		2.31	0.17	3.1		18.3	16	15d					
VBTU137	2008 EC155	1.92	0.21	2.0	0.52	21.8	8	1d	0.18	21.5	-4	189	0.55
		3.05	0.09	10.3		17.5	13	3d					
VBTU145	2008 DM83	2.33	0.18	4.0	0.93	18.7	8	1d	0.06	20.1	-4	189	0.61
		2.54	0.22	5.5		17.8	28	3y					
VBTU155	2001 SA350	2.48	0.15	3.4	1.12	18.6	8	1d	0.06	20.6	-4	189	0.60
		2.73	0.03	2.8		16.3	84	10y					
VBTU163	2008 EG145	3.03	0.04	2.6	1.92	17.0	6	1d	0.12	20.9	-3	162	0.47
VBTU174	2008 FQ65	2.26	0.49	3.5	0.18	18.4	2	1d	0.00	18.9	0	132	0.28
		2.58	0.14	13.2		17.4	25	72d					
VBTU212	2008 FX41	2.33	0.24	7.0	0.78	19.7	5	1d	0.14	20.4	1	172	0.65
		2.66	0.29	8.9		19.2	21	40d					
VBVI001	2005 SO198	2.53	0.03	1.0	1.45	17.4	14	1d	0.11	20.3	0	190	0.60
		2.63	0.18	1.5		17.2	44	5y					
VBVI002	2008 EZ127	2.33	0.17	7.7	0.93	18.8	14	1d	0.11	20.1	0	190	0.67
		2.54	0.13	11.8		17.8	28	28d					
VBVI004	2008 EU144	2.54	0.02	0.8	1.48	17.2	23	2d	0.18	20.3	0	190	0.58
		2.55	0.05	0.9		17.2	30	16d					
VBVI006	2008 EV144	2.80	0.22	2.6	1.19	18.4	15	1d	0.17	20.5	0	190	0.54

Table A.2 (continued) – Later identification of unknown asteroids observed at ESO/MPG.

Acronym	Designation	$a$	$e$	$i$	MOID	$H$	pos	arc	$rms$	$R$	$\beta$	$\epsilon$	$\mu$
VBVI009	2008 EZ145	3.08	0.04	1.9	1.94	16.6	22	2d	0.12	20.5	-1	190	0.50
		3.02	0.23	2.6		16.2	25	13d					
VBVI010	2008 EY33	2.66	0.22	3.1	1.07	17.2	22	2d	0.21	19.4	0	191	0.57
		2.53	0.12	3.2		17.8	56	15y					
VBVI011	2008 ET144	2.21	0.11	0.4	0.98	18.3	22	2d	0.09	19.9	0	190	0.61
		2.27	0.14	0.4		18.8	44	8y					
VBVI016	2002 TT318	2.38	0.11	6.8	1.12	18.2	8	1d	0.11	20.3	4	193	0.63
		2.57	0.24	12.6		17.4	28	7y					
VBVI021	2008 EY144	2.38	0.19	2.4	0.93	18.7	8	1d	0.08	20.2	4	193	0.55
VBVI024	2008 EX144	2.33	0.24	7.0	0.78	19.4	8	1d	0.17	20.4	4	192	0.59
		3.81	0.30	27.5		16.2	16	6d					
VBVI026	2008 CR152	2.69	0.05	24.9	1.57	15.8	8	1d	0.09	19.3	0	190	0.72
		2.64	0.06	22.1		16.3	52	28d					
VBVI035	2008 EA146	2.87	0.15	2.5	1.43	16.1	8	1d	0.07	20.5	0	191	0.53
VBVI039	2008 CG89	2.27	0.07	6.3	1.12	17.1	8	1d	0.09	19.1	-1	191	0.67
		2.24	0.10	5.7		17.6	41	35d					
VBVI041	2008 EB146	2.38	0.02	2.9	1.34	17.5	8	1d	0.07	20.1	-1	191	0.63
		2.41	0.14	2.7		18.2	18	25d					
VBVI042	2008 EW33	2.42	0.20	2.6	0.93	19.0	8	1d	0.04	20.4	0	191	0.57
		2.75	0.04	6.3		17.4	16	12d					
VBTV147	2003 SF319	2.18	0.14	2.2	0.89	20.1	7	1d	0.22	21.4	-4	189	0.64
		2.19	0.14	3.5		18.2	52	12y					

Table A.3: Outstanding unknown objects observed at ESO/MPG.

Acronym	$a$	$e$	$i$	MOID	$H$	pos	arc	$rms$	$R$	$\beta$	$\epsilon$	$\mu$
VB002	3.12	0.06	8.4	1.94	15.9	8	1d	0.16	21.1	0	123	0.09
VB003	2.38	0.11	3.0	1.11	17.7	8	1d	0.08	20.8	0	123	0.19
VB004	2.62	0.19	14.8	1.11	17.6	8	1d	0.16	20.6	0	124	0.38
VB005	3.03	0.29	2.1	1.13	17.1	7	1d	0.09	20.6	0	124	0.24
VB006	2.22	0.05	6.5	1.12	17.1	8	1d	0.10	20.6	0	124	0.11
VB007	2.29	0.16	1.1	0.92	18.2	8	1d	0.14	20.8	0	124	0.26
VB008	2.38	0.23	2.3	0.85	16.3	7	1d	0.16	20.9	0	124	0.10
VB010	2.85	0.23	2.3	1.17	17.0	8	1d	0.11	21.0	0	124	0.11
VB011	2.28	0.49	6.7	0.19	20.5	8	1d	0.13	20.8	0	124	0.55
VB012	2.41	0.21	4.0	0.91	16.6	7	1d	0.15	21.2	0	124	0.10
VB013	2.31	0.23	5.9	0.82	17.6	8	1d	0.09	20.8	0	124	0.10
VB015	2.47	0.05	6.0	1.35	17.0	8	1d	0.09	21.0	0	124	0.09
VB016	2.23	0.23	5.6	0.75	17.7	8	1d	0.09	21.0	0	124	0.12
VB017	2.41	0.21	3.4	0.91	16.5	8	1d	0.12	21.1	0	124	0.09
VB019	2.40	0.22	5.9	0.89	16.7	8	1d	0.18	21.2	-1	124	0.12
VB020	2.33	0.11	5.2	1.08	17.2	8	1d	0.22	21.3	-1	124	0.09
VB021	2.59	0.00	12.2	1.58	17.2	7	1d	0.28	21.3	-1	124	0.15
VB022	2.30	0.49	2.6	0.18	20.6	6	1d	0.09	20.8	-1	124	0.28
VB023	2.35	0.24	4.9	0.79	16.4	8	1d	0.17	21.0	-1	124	0.12
VB025	2.56	0.09	0.9	1.33	17.2	8	1d	0.07	20.8	-1	124	0.11
VB026	2.17	0.03	0.6	1.10	17.9	8	1d	0.08	21.0	-1	124	0.13
VB028	2.23	0.16	6.9	0.87	17.0	7	1d	0.15	21.0	0	124	0.09
VB030	2.51	0.07	1.5	1.33	17.5	7	1d	0.12	21.0	-1	123	0.11
VB031	2.36	0.10	2.7	1.13	16.7	7	1d	0.25	20.7	-1	125	0.07
VB032	2.34	0.18	2.1	0.92	18.8	7	1d	0.22	21.3	-1	126	0.25
VB033	2.67	0.09	1.6	1.44	16.2	6	1d	0.09	20.8	-1	125	0.07
VB034	2.34	0.11	6.9	1.08	—	4	1d	0.07	—	-1	125	0.10
VB035	2.54	0.02	9.5	1.49	17.4	6	1d	0.11	21.4	-1	126	0.15
VB038	2.16	0.02	0.7	1.10	18.1	7	1d	0.12	21.1	-1	126	0.08
VB040	2.59	0.00	8.2	1.59	17.2	7	1d	0.14	21.2	-1	126	0.14
VB041	2.29	0.02	8.9	1.25	17.4	7	1d	0.12	20.9	-1	126	0.18
VB042	2.45	0.05	5.5	1.33	17.8	7	1d	0.22	21.3	-1	126	0.13
VB043	2.69	0.08	1.3	1.47	16.7	6	1d	0.10	21.3	-1	126	0.08
VB044	2.62	0.55	2.2	0.18	20.5	7	1d	0.12	21.3	-1	126	0.20
VB046	2.21	0.13	6.7	0.93	19.3	7	1d	0.98	20.7	-1	191	0.68
VB048	2.27	0.15	4.1	0.92	18.7	8	1d	0.11	21.2	-1	126	0.22
VB049	3.02	0.09	14.2	1.74	16.2	8	1d	0.18	21.3	-1	126	0.16
VB050	3.12	0.06	1.6	1.94	15.9	8	1d	0.09	21.1	-1	127	0.09
VB051	2.70	0.04	3.8	1.59	17.2	7	1d	0.21	21.2	-1	127	0.07
VB052	2.62	0.11	3.2	1.33	16.7	8	1d	0.20	21.2	-1	126	0.10
VB053	2.27	0.14	6.6	0.94	17.1	8	1d	0.13	21.1	-1	126	0.14
VB054	2.52	0.16	0.6	1.11	18.3	8	1d	0.17	21.3	-1	126	0.14
VB055	2.23	0.22	5.5	0.77	17.9	8	1d	0.06	21.1	-1	126	0.15
VB056	2.40	0.03	7.3	1.33	17.7	8	1d	0.08	21.2	-1	126	0.15
VB058	3.16	0.19	2.2	1.56	15.5	8	1d	0.19	21.2	-1	126	0.13
VB059	2.50	0.04	4.0	1.40	17.2	8	1d	0.09	21.2	-1	126	0.09
VB060	2.49	0.04	0.9	1.39	17.0	7	1d	0.11	21.0	-1	126	0.05
VB061	2.61	0.00	3.4	1.59	16.8	8	1d	0.09	20.8	-2	126	0.08
VB062	2.39	0.20	3.8	0.92	18.1	8	1d	0.10	20.6	-1	126	0.27
VB063	2.27	0.07	5.3	1.11	18.0	8	1d	0.09	21.0	-1	126	0.18
VB064	2.47	0.18	2.1	1.03	16.8	8	1d	0.13	21.3	-1	126	0.11

Table A.3 (continued) – Outstanding unknown objects observed at ESO/MPG.

Acronym	$a$	$e$	$i$	MOID	$H$	pos	arc	$rms$	$R$	$\beta$	$\epsilon$	$\mu$
VB065	2.60	0.00	3.1	1.58	17.4	6	1d	0.10	21.4	-1	126	0.07
VBOP001	2.43	0.08	5.6	1.24	17.3	7	1d	0.14	20.3	-3	162	0.56
VBOP002	2.79	0.20	5.0	1.22	17.8	6	1d	0.11	20.2	-3	162	0.47
VBOP003	2.20	0.02	4.3	1.17	18.8	8	1d	0.24	21.1	-3	162	0.61
VBOP004	2.04	0.28	6.3	0.51	20.5	7	1d	0.47	21.0	-3	162	0.76
VBOP008	3.30	0.11	2.4	1.92	15.3	8	1d	0.12	19.6	-3	162	0.45
VBOP009	2.35	0.18	4.0	0.93	19.5	8	1d	0.15	21.0	-4	162	0.53
VBOP010	1.85	0.25	5.0	0.42	20.8	8	1d	0.48	20.8	-4	162	0.74
VBOP011	2.21	0.05	2.7	1.09	18.3	8	1d	0.18	21.0	-4	162	0.61
VBOP012	2.46	0.05	2.3	1.33	18.4	8	1d	0.15	21.1	-4	162	0.55
VBOP014	2.34	0.00	4.2	1.32	17.5	8	1d	0.08	20.2	-4	162	0.58
VBOP015	3.19	0.03	2.7	2.08	16.4	8	1d	0.18	21.0	-4	162	0.45
VBOP016	2.34	0.10	4.1	1.11	18.9	8	1d	0.10	21.0	-4	162	0.57
VBOP018	2.33	0.00	0.6	1.32	18.0	8	1d	0.09	20.7	0	163	0.60
VBOP019	2.30	0.13	3.1	1.00	16.7	8	1d	0.09	19.9	0	163	0.62
VBOP020	2.35	0.16	2.1	0.99	19.1	8	1d	0.09	20.8	0	163	0.56
VBOP021	2.73	0.05	4.5	1.60	17.5	8	1d	0.20	20.7	0	163	0.54
VBOP022	2.57	0.01	2.3	1.54	17.6	8	1d	0.10	20.8	0	163	0.56
VBOP025	2.31	0.09	4.3	1.11	17.5	6	1d	0.04	19.5	0	163	0.60
VBOP026	2.61	0.23	3.2	1.02	18.9	6	1d	0.24	20.7	0	163	0.50
VBOP027	2.40	0.20	2.1	0.93	19.1	8	1d	0.06	20.6	-1	163	0.53
VBOP028	2.50	0.07	0.8	1.33	17.8	8	1d	0.09	20.4	-1	163	0.56
VBOP029	2.34	0.22	3.3	0.82	19.6	8	1d	0.07	20.7	-1	163	0.52
VBOP030	2.12	0.01	1.7	1.11	18.5	8	1d	0.11	20.5	-1	163	0.64
VBOP031	2.84	0.03	3.8	1.77	17.1	8	1d	0.22	21.0	-1	163	0.52
VBOP032	2.69	0.25	4.2	1.03	19.0	7	1d	0.25	20.9	-1	163	0.48
VBSO002	2.09	0.10	5.2	0.90	19.4	14	1d	0.21	20.7	11	176	0.70
VBSO003	2.62	0.05	6.9	1.47	16.3	11	1d	0.09	19.6	11	176	0.60
VBSO005	2.01	0.20	4.2	0.63	20.2	11	1d	0.09	20.4	10	176	0.61
VBSO006	2.60	0.22	5.6	1.04	18.8	9	1d	0.08	20.5	11	176	0.56
VBSO009	2.35	0.10	7.1	1.12	18.6	8	1d	0.11	20.6	11	176	0.66
VBSO013	2.13	0.12	5.5	0.90	19.5	8	1d	0.15	20.7	10	176	0.69
VBSO015	2.70	0.08	14.0	1.47	16.0	9	1d	0.06	19.8	10	176	0.62
VBSO016	2.90	0.26	5.6	1.15	18.2	8	1d	0.05	20.2	10	176	0.53
VBSO017	3.14	0.05	11.5	1.98	16.4	8	1d	0.18	20.8	10	176	0.52
VBSO018	2.20	0.23	14.8	0.72	17.4	7	1d	0.36	20.7	10	176	0.73
VBSO019	1.94	0.22	3.6	0.52	21.1	8	1d	0.16	20.7	10	176	0.54
VBSO020	2.24	0.27	4.7	0.65	19.9	7	1d	0.08	20.2	10	176	0.53
VBSO021	2.40	0.20	2.8	0.93	19.4	7	1d	0.10	20.7	3	173	0.60
VBSO022	2.30	0.27	2.3	0.68	20.3	6	1d	0.17	20.6	3	173	0.52
VBSO023	2.79	0.09	1.8	1.54	17.5	7	1d	0.13	20.6	3	173	0.57
VBSO025	2.71	0.07	4.1	1.51	17.5	7	1d	0.12	20.7	3	173	0.58
VBSO026	3.15	0.19	2.8	1.54	15.6	7	1d	0.10	20.5	3	173	0.49
VBSO027	2.41	0.20	2.5	0.93	18.9	7	1d	0.05	20.1	3	173	0.59
VBSO028	2.14	0.12	3.1	0.89	19.5	6	1d	0.24	20.6	2	173	0.67
VBSO029	2.86	0.17	2.1	1.39	16.8	7	1d	0.11	20.6	2	173	0.56
VBSO030	2.54	0.19	2.0	1.07	18.7	7	1d	0.07	20.4	2	173	0.59
VBSO031	2.34	0.25	3.5	0.77	19.2	7	1d	0.09	19.9	2	173	0.60
VBSO032	2.95	0.01	2.5	1.92	16.9	6	1d	0.28	20.5	2	173	0.54
VBSO033	3.11	0.06	3.1	1.92	16.4	7	1d	0.10	20.0	3	173	0.52
VBSO034	2.29	0.22	8.4	0.79	16.9	7	1d	0.49	20.3	3	173	0.65



Table A.3 (continued) – Outstanding unknown objects observed at ESO/MPG.

Acronym	$a$	$e$	$i$	MOID	$H$	pos	arc	$rms$	$R$	$\beta$	$\epsilon$	$\mu$
VBSO035	2.48	0.10	10.8	1.23	18.4	4	1d	0.39	20.6	3	173	0.69
VBSO037	2.38	0.17	5.4	0.96	16.6	7	1d	0.09	20.0	3	173	0.64
VBSO038	2.72	0.17	22.1	1.38	16.9	7	1d	0.11	20.4	3	173	0.70
VBSO039	2.26	0.07	6.0	1.10	17.1	8	1d	0.14	20.3	2	117	0.30
VBSO040	2.69	0.03	7.7	1.59	16.0	8	1d	0.09	20.2	2	117	0.19
VBSO041	2.25	0.06	2.0	1.10	16.5	6	1d	0.05	19.7	2	117	0.28
VBSO042	2.61	0.00	6.8	1.59	16.1	7	1d	0.23	20.3	2	117	0.14
VBSO043	2.21	0.05	2.6	1.10	16.4	7	1d	0.13	20.1	2	117	0.16
VBSO044	2.76	0.19	4.4	1.23	18.0	8	1d	0.08	20.4	2	163	0.51
VBSO045	3.19	0.05	1.7	2.03	16.3	6	1d	0.22	20.3	2	163	0.49
VBSO046	2.74	0.19	4.3	1.22	18.1	8	1d	0.08	20.5	2	163	0.51
VBSO047	2.47	0.06	11.5	1.34	15.7	8	1d	0.17	18.7	2	163	0.63
VBSO048	1.90	0.21	1.5	0.51	20.9	8	1d	0.14	20.6	2	163	0.49
VBSO049	2.30	0.01	6.0	1.27	17.5	8	1d	0.07	20.2	2	163	0.63
VBSO050	2.10	0.11	1.0	0.88	18.7	8	1d	0.12	20.1	2	164	0.62
VBSO051	2.80	0.20	1.7	1.26	18.1	8	1d	0.16	20.6	2	163	0.51
VBSO053	2.39	0.12	5.3	1.11	17.7	7	1d	0.04	19.7	2	164	0.59
VBSO054	2.27	0.22	4.6	0.77	19.5	8	1d	0.07	20.4	2	164	0.55
VBSO055	2.41	0.15	7.1	1.05	18.1	6	1d	0.36	20.0	2	164	0.61
VBSO056	2.54	0.26	2.1	0.88	19.2	8	1d	0.08	20.5	2	163	0.49
VBSO057	2.87	0.02	2.1	1.81	16.5	8	1d	0.11	20.3	2	163	0.51
VBSO058	2.48	0.06	2.9	1.33	17.8	8	1d	0.07	20.4	2	163	0.57
VBSO060	2.45	0.26	3.7	0.83	18.5	6	1d	0.05	19.7	2	163	0.53
VBSO061	2.50	0.04	3.2	1.39	17.2	6	1d	0.07	20.4	2	163	0.57
VBSO062	2.32	0.09	3.7	1.11	18.1	6	1d	0.13	20.2	2	163	0.59
VBSO064	2.30	0.27	4.5	0.68	20.2	8	1d	0.12	20.7	11	184	0.51
VBSO065	2.98	0.24	8.3	1.29	18.1	8	1d	0.18	20.5	11	184	0.55
VBSO067	2.22	0.26	4.5	0.66	20.3	8	1d	0.14	20.6	11	184	0.53
VBSO069	2.27	0.22	4.8	0.78	19.7	7	1d	0.30	20.6	11	184	0.57
VBSO070	2.35	0.01	6.2	1.33	17.0	5	1d	0.09	19.6	11	184	0.65
VBSO071	3.04	0.22	9.9	1.39	17.9	7	1d	0.25	20.6	11	184	0.55
VBSO072	1.95	0.13	17.5	0.70	19.4	8	1d	0.12	20.0	11	184	1.17
VBSO073	2.21	0.01	6.9	1.18	18.3	8	1d	0.26	20.5	11	184	0.69
VBSO074	2.24	0.27	5.2	0.66	20.5	8	1d	0.27	20.9	11	184	0.53
VBSO075	2.20	0.14	5.4	0.90	19.4	8	1d	0.19	20.7	11	184	0.64
VBSO076	2.31	0.17	5.5	0.94	19.2	5	1d	0.38	20.7	11	184	0.62
VBSO077	2.11	0.12	7.0	0.85	18.3	4	1d	0.10	20.6	11	184	0.73
VBSO078	2.43	0.28	5.0	0.78	19.8	5	1d	0.31	20.6	11	184	0.53
VBSO079	2.64	0.10	7.2	1.38	17.5	5	1d	0.35	21.1	11	184	0.56
VBTO003	2.22	0.10	1.8	1.01	18.6	14	1d	0.18	20.6	-3	161	0.58
VBTO004	2.57	0.25	2.8	0.91	16.3	14	1d	0.13	20.6	-3	161	0.52
VBTO007	2.33	0.35	9.1	0.56	18.5	11	1d	0.65	20.8	-3	162	0.76
VBTO009	2.27	0.15	7.0	0.93	19.2	12	1d	0.44	20.8	-4	162	0.59
VBTO014	2.40	0.16	8.1	1.04	18.9	13	1d	0.26	20.9	-4	162	0.57
VBTO016	1.40	0.15	1.7	0.20	22.7	14	1d	0.87	20.6	-4	161	0.68
VBTO017	3.07	0.15	3.4	1.60	17.1	14	1d	0.17	20.5	-3	161	0.46
VBTO018	2.40	0.12	3.1	1.11	17.8	14	1d	0.27	20.0	-3	161	0.53
VBTO020	2.32	0.09	3.3	1.11	17.5	8	1d	0.14	19.6	-3	162	0.56
VBTO026	2.26	0.11	1.8	1.02	18.9	8	1d	0.11	20.9	-3	162	0.58
VBTO030	2.34	0.18	4.0	0.93	19.4	8	1d	0.12	21.0	-4	162	0.53
VBTO031	2.47	0.22	3.5	0.93	19.3	8	1d	0.11	20.9	-4	162	0.47

Table A.3 (continued) – Outstanding unknown objects observed at ESO/MPG.

Acronym	$a$	$e$	$i$	MOID	$H$	pos	arc	$rms$	$R$	$\beta$	$\epsilon$	$\mu$
VBTO032	2.23	0.16	1.9	0.87	19.5	8	1d	0.21	20.9	-4	162	0.55
VBTO033	2.50	0.19	6.1	1.02	19.1	8	1d	0.16	21.0	-4	162	0.53
VBTO034	1.93	0.17	3.2	0.61	20.3	8	1d	0.49	20.7	-4	162	0.54
VBTO037	2.30	0.19	7.0	0.87	19.6	8	1d	0.14	21.1	-4	162	0.61
VBTO041	2.33	0.22	3.2	0.82	19.8	8	1d	0.13	21.1	-4	162	0.48
VBTO042	2.34	0.10	5.6	1.11	19.0	8	1d	0.17	21.1	-4	162	0.56
VBTO048	2.22	0.18	6.6	0.82	19.8	7	1d	0.47	21.0	-3	162	0.61
VBTO050	3.08	0.25	3.2	1.30	18.1	8	1d	0.16	20.9	-3	162	0.45
VBTO053	2.31	0.21	2.3	0.82	19.7	8	1d	0.12	20.9	-3	162	0.51
VBTOb10	2.22	0.05	2.5	1.10	18.2	8	1d	0.15	20.9	-4	162	0.60
VBTOb13	2.49	0.06	3.6	1.33	17.9	16	1d	0.11	20.5	-4	162	0.52
VBTO003	2.40	0.13	4.2	1.11	19.1	14	1d	0.32	21.1	-5	192	0.59
VBTO004	2.30	0.16	5.5	0.93	19.8	3	1d	0.16	21.3	-5	192	0.62
VBTO007	2.39	0.12	5.4	1.12	18.7	4	1d	0.13	20.7	-6	192	0.62
VBTO009	2.88	0.25	15.8	1.17	16.1	5	1d	0.15	20.9	-5	192	0.53
VBTO010	2.29	0.19	4.6	0.84	18.6	4	1d	0.09	20.8	-6	192	0.69
VBTO021	2.60	0.35	6.7	0.72	18.4	15	1d	0.14	20.5	-3	161	0.66
VBTO022	2.22	0.32	5.2	0.54	18.3	14	1d	0.20	18.9	-3	161	0.64
VBTO026	1.97	0.36	18.7	0.24	17.5	6	1d	0.57	20.8	-6	193	0.78
VBTO031	1.88	0.38	19.1	0.17	18.0	4	1d	0.53	21.1	-6	192	0.84
VBTO032	1.99	0.30	16.8	0.39	17.9	5	1d	0.67	21.1	-6	192	0.87
VBTO036	2.33	0.00	3.8	1.31	18.8	5	1d	0.24	21.4	-6	192	0.62
VBTO040	2.47	0.16	6.6	1.06	17.0	14	1d	0.23	20.7	-3	161	0.55
VBTO042	2.39	0.19	4.5	0.93	19.1	8	1d	0.33	20.7	-3	161	0.51
VBTO043	1.92	0.25	1.4	0.44	21.4	14	1d	0.08	20.6	-4	188	0.49
VBTO046	2.72	0.05	3.3	1.59	17.7	14	1d	0.12	20.9	-4	188	0.57
VBTO051	2.38	0.11	5.4	1.12	19.3	10	1d	0.18	21.2	-4	188	0.65
VBTO053	2.77	0.05	2.8	1.62	17.5	10	2d	0.39	21.2	-4	189	0.54
VBTO067	2.77	0.27	3.3	1.04	19.6	13	1d	0.24	21.2	-4	188	0.55
VBTO081	2.31	0.01	2.9	1.27	18.2	3	1d	0.10	20.8	-5	189	0.65
VBTO082	2.74	0.05	9.7	1.61	18.2	3	1d	0.04	21.4	-4	189	0.60
VBTO084	1.98	0.06	9.2	0.85	19.4	3	1d	0.24	21.3	-5	189	0.79
VBTO086	2.77	0.06	4.0	1.61	18.3	3	1d	0.10	21.5	-4	189	0.56
VBTO087	2.22	0.13	9.0	0.93	19.5	3	1d	0.18	21.4	-4	189	0.74
VBTO088	2.45	0.22	2.2	0.93	20.1	3	1d	0.16	21.4	-4	189	0.56
VBTO091	2.12	0.10	2.5	0.89	18.4	4	1d	0.07	20.9	-4	189	0.71
VBTO093	2.36	0.01	6.4	1.33	18.3	4	1d	0.05	20.8	-4	189	0.66
VBTO094	2.06	0.16	5.5	0.75	18.5	9	1d	0.20	21.1	9	135	0.22
VBTO095	3.19	0.08	17.1	1.92	16.2	13	1d	0.21	20.7	9	135	0.19
VBTO096	2.42	0.50	7.7	0.26	20.4	12	1d	0.20	21.1	9	135	0.51
VBTO097	2.48	0.05	7.1	1.37	14.7	9	1d	0.21	18.6	9	135	0.24
VBTO099	1.95	0.13	4.8	0.70	17.5	14	1d	0.03	19.6	9	135	0.23
VBTO100	2.28	0.02	6.1	1.23	17.3	14	1d	0.09	20.6	9	135	0.19
VBTO102	2.27	0.03	6.6	1.21	17.5	14	1d	0.14	20.8	9	135	0.17
VBTO105	2.78	0.17	19.6	1.31	16.3	13	1d	0.24	20.6	-3	161	0.57
VBTO106	2.36	0.19	5.8	0.93	19.1	10	1d	0.19	20.7	-3	161	0.51
VBTO109	2.35	0.14	1.7	1.04	17.6	13	1d	0.07	19.6	0	162	0.55
VBTO111	2.33	0.31	3.2	0.63	19.0	13	1d	0.20	20.4	0	162	0.64
VBTO112	2.39	0.12	0.5	1.11	17.6	13	1d	0.10	19.7	0	163	0.53
VBTO114	2.44	0.21	2.9	0.93	18.2	11	1d	0.07	19.7	-1	163	0.50
VBTO115	2.45	0.28	1.3	0.77	18.9	11	1d	0.08	20.0	-1	163	0.41

Table A.3 (continued) – Outstanding unknown objects observed at ESO/MPG.

Acronym	$a$	$e$	$i$	MOID	$H$	pos	arc	$rms$	$R$	$\beta$	$\epsilon$	$\mu$
VBTU116	2.43	0.13	3.6	1.11	18.7	6	1d	0.15	20.8	-1	163	0.53
VBTU117	2.22	0.13	7.4	0.93	19.1	11	1d	0.19	20.7	-1	163	0.62
VBTU118	2.21	0.17	4.2	0.83	17.4	13	1d	0.19	20.7	-1	163	0.62
VBTU120	2.54	0.02	2.5	1.48	16.3	10	1d	0.07	19.6	-1	162	0.54
VBTU121	2.39	0.08	11.6	1.21	17.9	10	1d	0.72	20.9	-1	162	0.59
VBTU122	2.54	0.07	3.9	1.35	17.7	12	1d	0.22	20.8	-1	162	0.53
VBTU126	2.32	0.01	2.3	1.30	18.1	12	1d	0.14	20.8	-1	162	0.58
VBTU127	3.12	0.07	2.4	1.92	16.9	12	1d	0.18	20.8	-1	162	0.46
VBTU129	2.32	0.17	5.1	0.93	19.0	12	1d	0.20	20.6	0	162	0.55
VBTU130	2.36	0.11	3.2	1.11	18.5	9	1d	0.25	20.6	0	162	0.55
VBTU131	3.07	0.05	3.3	1.92	17.1	8	1d	0.42	21.0	0	162	0.47
VBTU132	2.31	0.12	22.7	1.09	17.6	5	1d	0.95	21.1	-28	183	0.70
VBTU133	2.32	0.12	22.8	1.10	17.5	8	1d	0.49	21.0	-28	183	0.70
VBTU140	2.22	0.17	4.7	0.84	17.2	8	1d	0.05	20.4	-4	189	0.67
VBTU142	2.73	0.05	2.5	1.61	18.3	6	1d	0.24	21.5	-4	189	0.56
VBTU143	2.10	0.30	3.6	0.47	18.8	3	1d	0.75	21.7	-4	189	0.75
VBTU144	2.37	0.25	4.5	0.78	20.6	6	1d	0.20	21.4	-4	189	0.56
VBTU146	2.50	0.07	3.6	1.34	18.3	8	1d	0.10	20.9	-4	189	0.60
VBTU148	2.46	0.28	2.7	0.78	20.6	8	1d	0.21	21.4	-4	189	0.50
VBTU151	2.35	0.25	2.8	0.74	18.0	8	1d	0.13	21.3	-4	189	0.67
VBTU152	2.61	0.22	9.3	1.04	19.6	8	1d	0.39	21.3	-4	189	0.66
VBTU156	2.36	0.25	2.1	0.78	20.7	7	1d	0.20	21.5	-4	189	0.53
VBTU162	2.36	0.08	3.9	1.18	18.5	8	1d	0.08	20.9	-3	162	0.57
VBTU164	2.42	0.04	3.1	1.33	18.2	5	1d	0.22	20.9	-3	162	0.55
VBTU166	2.44	0.07	6.5	1.28	17.3	7	1d	0.24	21.2	1	132	0.17
VBTU167	2.26	0.15	6.8	0.93	17.3	7	1d	0.28	21.2	1	132	0.21
VBTU168	2.24	0.16	7.0	0.89	17.4	8	1d	0.18	21.3	1	132	0.21
VBTU169	2.74	0.15	13.8	1.33	18.1	6	1d	0.13	21.5	0	132	0.27
VBTU170	2.78	0.24	16.0	1.11	18.2	8	1d	0.21	21.0	0	132	0.40
VBTU171	2.42	0.07	1.4	1.25	17.4	8	1d	0.20	21.3	0	132	0.15
VBTU172	2.29	0.08	3.6	1.11	17.8	8	1d	0.13	20.7	0	132	0.10
VBTU173	2.38	0.02	1.2	1.33	17.5	8	1d	0.14	20.8	0	132	0.09
VBTU175	2.46	0.18	7.5	1.01	16.6	6	1d	0.23	21.1	0	132	0.22
VBTU176	2.61	0.12	10.6	1.31	16.4	8	1d	0.17	20.9	0	132	0.21
VBTU177	2.27	0.03	7.0	1.21	17.6	6	1d	0.19	21.0	0	132	0.17
VBTU178	3.11	0.06	2.0	1.93	16.0	6	1d	0.16	21.1	0	132	0.16
VBTU179	2.43	0.07	0.6	1.26	17.1	5	1d	0.20	21.0	0	132	0.15
VBTU180	2.37	0.11	7.1	1.11	16.5	8	1d	0.09	19.4	0	132	0.16
VBTU181	3.04	0.09	2.2	1.78	15.8	3	1d	0.09	20.9	0	132	0.17
VBTU183	2.37	0.10	5.2	1.14	17.4	4	1d	0.11	21.3	0	132	0.18
VBTU184	2.20	0.18	7.3	0.81	17.4	7	1d	0.21	21.3	0	132	0.22
VBTU188	2.68	0.22	9.2	1.09	16.7	8	1d	0.09	20.9	11	135	0.27
VBTU189	2.93	0.26	11.3	1.18	15.9	7	1d	0.08	20.7	10	136	0.22
VBTU190	2.42	0.04	7.6	1.34	16.4	7	1d	0.09	19.7	10	136	0.19
VBTU191	3.15	0.24	11.8	1.40	16.3	7	1d	0.08	21.1	10	136	0.20
VBTU192	2.01	0.14	5.7	0.74	18.9	7	1d	0.09	21.0	10	136	0.22
VBTU193	3.40	0.24	14.2	1.59	16.1	7	1d	0.12	20.9	11	136	0.19
VBTU194	2.21	0.18	7.1	0.84	17.7	8	1d	0.18	21.5	10	136	0.30
VBTU195	2.30	0.46	5.3	0.26	21.5	7	1d	0.17	21.3	10	135	0.47
VBTU196	2.20	0.06	8.5	1.08	17.9	8	1d	0.13	21.2	10	135	0.32
VBTU197	3.02	0.68	8.2	0.09	18.9	7	1d	0.38	21.4	10	135	0.68

Table A.3 (continued) – Outstanding unknown objects observed at ESO/MPG.

Acronym	$a$	$e$	$i$	MOID	$H$	pos	arc	$rms$	$R$	$\beta$	$\epsilon$	$\mu$
VB TU198	2.42	0.04	6.9	1.34	18.2	6	1d	0.17	21.5	10	135	0.20
VB TU200	2.42	0.07	7.5	1.25	17.2	8	1d	0.10	21.1	0	132	0.18
VB TU201	2.66	0.10	10.2	1.41	16.1	14	1d	0.09	20.6	1	132	0.20
VB TU205	2.25	0.06	5.0	1.11	18.4	7	1d	0.41	21.3	0	132	0.11
VB TU206	2.38	0.51	1.3	0.19	20.6	4	1d	0.87	21.3	0	131	0.28
VB TU209	2.39	0.12	4.6	1.11	19.3	4	1d	0.26	21.2	1	171	0.63
VB TU210	2.89	0.01	2.1	1.85	17.0	5	1d	0.10	20.6	1	172	0.54
VB TU211	2.44	0.04	3.7	1.34	18.5	5	1d	0.14	20.9	1	172	0.63
VB TU214	2.22	0.17	2.0	0.84	17.7	5	1d	0.07	20.7	1	172	0.68
VB TU215	2.64	0.02	3.3	1.60	17.5	5	1d	0.12	20.5	1	171	0.59
VB TU216	3.16	0.04	11.3	2.02	16.4	5	1d	0.06	20.7	1	171	0.52
VB TU217	2.75	0.06	5.2	1.58	16.9	4	1d	0.09	20.6	1	171	0.57
VB TU218	3.05	0.04	8.8	1.92	17.2	4	1d	0.03	20.9	1	171	0.54
VB TU219	2.61	0.01	2.6	1.59	17.6	4	1d	0.15	20.6	1	171	0.59
VB TU220	2.38	0.08	2.1	1.17	18.1	5	1d	0.22	21.1	1	171	0.65
VB TU221	2.54	0.02	2.7	1.47	18.1	4	1d	0.09	21.1	1	171	0.60
VB TU222	1.01	0.08	2.2	0.03	24.7	5	1d	0.16	20.4	10	162	2.12
VB TU223	2.23	0.26	5.3	0.66	19.6	5	1d	0.36	20.9	10	162	0.63
VB TU225	2.23	0.27	4.8	0.65	19.8	4	1d	0.25	21.1	10	162	0.63
VB TU226	1.94	0.20	25.7	0.56	18.2	5	1d	0.52	21.0	10	162	0.89
VB TU227	2.47	0.10	6.1	1.22	18.4	5	1d	0.19	20.9	10	162	0.54
VB TU228	2.28	0.16	5.1	0.94	19.1	5	1d	0.07	20.7	10	162	0.53
VB TU229	2.60	0.07	11.2	1.43	17.2	7	1d	0.17	20.2	-17	188	0.58
VB TU230	2.54	0.03	14.8	1.52	17.3	6	1d	0.46	20.6	-17	188	0.58
VB TU231	2.80	0.14	13.1	1.42	17.4	5	1d	0.16	21.4	-1	126	0.18
VB TU232	1.94	0.20	0.8	0.58	18.3	8	1d	0.08	21.0	-1	126	0.07
VB TU233	2.34	0.11	5.9	1.08	17.2	8	1d	0.20	21.2	0	126	0.09
VB TU234	2.56	0.02	3.5	1.52	17.1	8	1d	0.09	21.1	0	126	0.04
VB TU235	2.70	0.04	4.1	1.59	17.4	5	1d	0.15	21.5	0	126	0.07
VB TU236	2.54	0.02	8.6	1.49	16.7	3	1d	0.17	20.7	0	126	0.12
VB TU237	2.52	0.16	3.8	1.13	16.8	8	1d	0.35	21.3	-1	126	0.11
VB TU238	2.36	0.10	5.9	1.12	16.7	8	1d	0.06	20.7	0	126	0.11
VB TU239	2.11	0.23	0.4	0.63	17.9	8	1d	0.09	21.2	-1	126	0.11
VB TU240	2.06	0.18	4.7	0.71	18.4	6	1d	0.16	21.2	-1	126	0.09
VB TU241	2.25	0.15	6.4	0.92	17.1	8	1d	0.18	21.1	-1	126	0.11
VB TU242	2.97	0.13	11.5	1.59	17.2	8	1d	0.14	21.3	-1	126	0.19
VB TU243	2.68	0.09	2.4	1.45	16.1	8	1d	0.09	20.7	-1	126	0.08
VB TU244	2.26	0.03	6.0	1.19	17.3	8	1d	0.10	20.8	-1	126	0.09
VB TU245	2.53	0.08	13.1	1.33	17.7	8	1d	0.25	21.2	-1	126	0.22
VB TU246	2.98	0.11	0.6	1.66	15.6	8	1d	0.07	20.8	-1	126	0.10
VB TU247	2.61	0.11	3.2	1.33	17.2	8	1d	0.10	20.7	-1	126	0.08
VB TU248	2.41	0.12	3.0	1.11	17.9	8	1d	0.10	20.9	-1	126	0.16
VB TU b61	2.29	0.22	12.0	0.79	17.7	4	1d	0.14	21.2	-4	189	0.69
VB VA002	2.50	0.39	13.8	0.57	17.8	3	1d	0.08	19.8	24	154	0.60
VB VA003	2.84	0.25	1.4	1.12	17.7	8	1d	0.12	21.1	-1	126	0.17
VB VI005	2.92	0.25	3.0	1.19	18.2	14	1d	0.12	20.4	0	190	0.52
VB VI007	2.64	0.20	14.6	1.12	18.3	11	1d	0.17	20.2	0	190	0.73
VB VI008	2.70	0.25	5.7	1.04	18.2	8	1d	0.50	19.9	0	190	0.56
VB VI012	2.38	0.18	11.5	0.96	16.8	7	1d	0.09	20.4	4	192	0.64
VB VI013	2.35	0.25	6.1	0.76	17.4	7	1d	0.26	18.8	4	192	0.67
VB VI014	2.20	0.06	8.0	1.08	18.2	7	1d	0.28	20.4	4	192	0.69

Table A.3 (continued) – Outstanding unknown objects observed at ESO/MPG.

Acronym	$a$	$e$	$i$	MOID	$H$	pos	arc	$rms$	$R$	$\beta$	$\epsilon$	$\mu$
VBVI015	2.39	0.20	7.1	0.93	19.0	7	1d	0.12	20.5	4	192	0.62
VBVI017	2.41	0.18	3.4	0.99	19.1	8	1d	0.14	20.8	4	193	0.58
VBVI018	2.40	0.20	2.9	0.93	18.8	8	1d	0.12	20.3	4	193	0.54
VBVI019	2.64	0.01	12.9	1.60	16.1	8	1d	0.07	19.3	3	193	0.63
VBVI020	2.40	0.20	2.1	0.93	19.3	7	1d	0.12	20.8	4	193	0.54
VBVI022	2.26	0.27	7.9	0.65	19.1	8	1d	0.28	19.9	4	192	0.74
VBVI023	2.55	0.17	14.5	1.12	16.8	8	1d	0.07	18.9	4	192	0.71
VBVI027	2.24	0.07	8.0	1.09	18.6	8	1d	0.57	20.5	0	190	0.69
VBVI029	2.24	0.08	8.0	1.07	18.6	8	1d	0.58	20.4	0	191	0.69
VBVI030	2.27	0.20	0.2	0.82	19.4	7	1d	0.14	20.4	0	191	0.59
VBVI031	2.45	0.19	2.3	0.97	16.8	8	1d	0.08	20.6	0	191	0.61
VBVI032	2.50	0.12	5.5	1.20	16.7	8	1d	0.06	20.2	0	191	0.61
VBVI033	2.00	0.21	4.2	0.59	20.4	8	1d	0.60	20.7	0	191	0.69
VBVI034	2.28	0.16	7.5	0.93	19.1	7	1d	0.08	20.5	0	191	0.67
VBVI036	2.86	0.29	3.4	1.04	18.6	8	1d	0.10	20.3	0	191	0.50
VBVI038	2.01	0.21	4.2	0.59	20.2	8	1d	0.56	20.5	-1	191	0.69
VBVI040	2.41	0.23	2.2	0.84	17.8	8	1d	0.10	20.8	-1	191	0.67
VBVI044	2.37	0.21	7.3	0.89	18.9	8	1d	0.55	20.5	0	190	0.69
VBVI213	2.45	0.57	2.0	0.07	25.3	5	1d	0.31	20.0	-1	191	7.17

Table A.4: Later identification of unknown asteroids observed with Swope telescope. First line represent our data and second line reffers to updated MPC data.

Acronym	Designation	$a$	$e$	$i$	MOID	$H$	pos	arc	$rms$	$R$	$\beta$	$\epsilon$	$\mu$
PBS007	2008 UC335	2.44	0.27	3.2	0.78	19.3	5	1d	0.27	19.9	1	182	0.53
		2.14	0.25	1.9		20.2	11	18d					
PBS009	2008 UE35	2.27	0.09	5.2	1.07	17.1	8	1d	0.22	19.8	0	182	0.67
		2.21	0.1	3.1		18.3	30	36d					
PBS015	2008 SM192	2.38	0.23	3.7	0.83	18.6	10	1d	0.22	19.5	-7	175	0.59
		2.8	0.14	5.4		16.9	20	30d					
PBT010	2008 TZ101	2.48	0.17	1.7	1.06	18.0	7	1d	0.12	19.8	0	188	0.59
		2.42	0.19	1.5		18.5	38	48d					
PBT012	2008 UZ25	2.33	0.24	4.6	0.77	19.0	3	1d	0.19	19.8	0	188	0.57
		3.1	0.19	12.2		17	18	35d					
PBT021	2008 UL55	2.13	0.13	0.7	0.86	18.5	6	1d	0.33	20.0	0	197	0.56
		2.37	0.12	1		17.2	79	12y					
PBT023	2008 TW81	2.44	0.19	0.4	0.99	18.4	5	1d	0.20	20.1	0	197	0.49
		2.99	0.11	1.6		17.2	24	35d					
PBT025	1998 UB46	2.65	0.24	3.7	1.03	18.1	10	1d	0.13	19.8	-3	187	0.55
		2.9	0.17	5.4		17.4	31	11y					

Table A.5: Outstanding unknown objects observed with Swope telescope.

Acronym	$a$	$e$	$i$	MOID	$H$	pos	arc	$rms$	$R$	$\beta$	$\epsilon$	$\mu$
PBS001	2.20	0.21	4.1	0.74	19.5	6	1d	0.23	20.5	-7	194	0.52
PBS002	2.44	0.24	3.6	0.85	19.3	6	1d	0.14	20.6	-7	194	0.46
PBS003	2.40	0.13	4.2	1.10	18.3	6	1d	0.18	20.4	-7	194	0.53
PBS004	2.50	0.16	9.4	1.15	18.0	6	1d	0.28	20.4	-8	194	0.59
PBS005	2.20	0.21	4.3	0.74	18.8	6	1d	0.07	19.8	-8	194	0.52
PBS006	2.49	0.03	5.4	1.42	17.2	8	1d	0.25	19.9	1	182	0.62
PBS008	2.72	0.18	6.0	1.23	17.2	8	1d	0.15	19.3	0	182	0.60
PBS010	2.24	0.19	6.1	0.83	18.8	8	1d	0.17	20.3	-12	153	0.46
PBS011	2.25	0.22	7.7	0.78	17.8	6	1d	0.11	19.1	-17	197	0.49
PBS014	2.97	0.16	13.5	1.49	14.9	10	1d	0.19	19.5	-7	175	0.54
PBS016	2.37	0.07	10.4	1.21	16.8	8	1d	0.32	19.7	-7	175	0.68
PBS017	2.77	0.04	4.8	1.66	16.5	10	1d	0.48	19.6	-8	175	0.59
PBT001	2.72	0.03	24.0	1.65	15.6	12	1d	0.16	19.1	-12	174	0.71
PBT002	2.91	0.18	10.1	1.40	16.5	4	1d	0.40	19.2	-12	174	0.57
PBT006	2.20	0.05	4.9	1.09	16.4	5	1d	0.33	19.9	4	-108	0.57
PBT007	2.30	0.01	5.3	1.27	17.0	4	1d	0.27	20.0	-7	-149	0.37
PBT008	2.33	0.22	3.1	0.82	19.1	3	1d	0.43	20.1	0	188	0.57
PBT009	2.72	0.32	0.5	0.85	15.3	7	1d	0.36	20.1	0	188	0.54
PBT011	2.06	0.16	4.3	0.74	18.8	8	1d	0.16	19.5	0	188	0.66
PBT013	2.82	0.27	2.8	1.06	18.4	3	1d	0.31	20.2	0	188	0.52
PBT014	2.21	0.15	3.2	0.89	18.9	6	1d	0.28	20.0	-3	184	0.65
PBT015	2.74	0.30	3.8	0.91	15.1	6	1d	0.14	19.8	-3	184	0.55
PBT016	2.14	0.12	2.3	0.89	18.9	6	1d	0.34	20.1	-3	184	0.66
PBT017	2.32	0.21	7.9	0.85	19.0	4	1d	0.21	20.2	-3	184	0.72
PBT018	3.08	0.02	2.1	2.04	16.0	6	1d	0.17	19.9	-3	184	0.51
PBT022	2.28	0.24	4.3	0.72	16.4	6	1d	0.45	20.1	0	197	0.58
PBT024	2.40	0.20	0.7	0.93	18.7	3	1d	0.42	20.3	0	197	0.46
PBT026	2.49	0.23	2.6	0.93	18.7	9	1d	0.22	20.0	-3	187	0.55
PBT027	2.67	0.09	6.2	1.42	16.7	9	1d	0.30	19.9	-3	187	0.59
PBT028	2.40	0.19	3.7	0.95	16.4	6	1d	0.46	20.0	-1	196	0.56
PBV002	2.15	0.15	2.3	0.84	18.4	4	1d	0.22	19.2	-5	176	0.68
PBV003	2.35	0.22	3.2	0.83	15.8	4	1d	0.34	19.3	-5	176	0.64
PBV004	2.30	0.40	2.4	0.37	19.7	4	1d	0.40	19.5	-5	176	0.60

Table A.6: Later identification of unknown asteroids observed at the INT. First line represent our data and second line reffers to updated MPC data.

Acronym	Designation	$a$	$e$	$i$	MOID	$H$	pos	arc	$rms$	$R$	$\beta$	$\epsilon$	$\mu$
VDT070	247902	2.30	0.08	6.4	1.12	17.8	4	1d	0.19	20.3	10	151	0.37
		2.86	0.20	9.0		16.3	51	10y					
VDT072	2005 YW147	2.38	0.11	6.3	1.12	17.3	5	1d	0.41	19.7	10	151	0.39
		2.42	0.15	5.8		17.6	33	6y					
VDT073	2008 SZ203	2.43	0.13	2.7	1.12	17.8	2	1d	0.00	19.7	5	173	0.61
		2.52	0.06	3.4		17.2	30	3y					
VIT003	2005 TO93	2.77	0.06	6.5	1.60	16.2	4	1d	0.42	20.4	4	240	0.17
		2.60	0.10	8.3		16.9	53	14y					
VIT005	2000 SN27	1.58	0.13	6.0	0.38	19.9	4	1d	0.38	19.0	-9	167	0.95
		2.66	0.20	14.0		16.2	78	10y					
VTD001	2010 CD146	2.40	0.20	3.9	0.93	18.2	4	1d	0.16	19.6	6	193	0.57
		2.76	0.09	4.0		16.7	11	11d					
VTD003	2010 CJ33	1.40	0.03	2.1	0.35	20.0	4	1d	0.56	19.3	6	193	1.15
		2.43	0.13	3.3		17.9	11	11d					
VTD004	2001 TY142	2.34	0.30	5.8	0.67	18.5	4	1d	0.19	18.9	14	183	0.49
		3.20	0.13	10.3		14.9	50	10y					
VTD012	2010 CU38	2.40	0.20	6.5	0.93	18.1	5	1d	0.28	19.2	0	178	0.67
		2.29	0.14	7.4		18.3	18	11d					
VTD025	2004 RJ308	2.15	0.08	9.0	0.98	17.5	5	1d	0.41	19.6	0	178	0.78
		2.37	0.18	9.6		17.0	29	18y					
VTD027	241531	2.44	0.02	0.9	1.38	16.4	5	1d	0.38	19.1	0	178	0.63
		2.68	0.04	7.5		16.2	63	11y					
VTD067	2003 UJ281	2.35	0.01	7.4	1.33	17.8	4	1d	0.16	20.8	10	151	0.43
		2.85	0.20	9.0		16.3	51	10y					
VTD073	2007 UN95	2.14	0.09	1.5	0.95	16.8	3	1d	0.89	20.8	-2	106	0.39
		2.78	0.08	2.6		16.1	33	4y					
VTU006	2009 BC142	2.50	0.19	2.2	1.05	18.6	6	1d	0.48	20.1	4	183	0.58
		2.71	0.09	4.5		16.8	25	10y					
VTU008	2009 BF55	2.33	0.22	5.4	0.83	18.9	4	1d	0.19	19.9	1	189	0.65
		3.16	0.14	16.2		16.8	19	40d					
VTU010	2009 BR86	2.41	0.20	3.5	0.94	18.1	5	1d	0.19	19.5	1	189	0.59
		2.81	0.14	5.7		16.7	31	4y					
VTU013	2010 JR112	2.57	0.03	4.2	1.50	16.8	8	1d	0.18	19.6	7	182	0.62
		2.55	0.28	4.9		15.7	59	6y					
VTU017	2009 BS86	2.49	0.15	3.6	1.12	18.0	5	1d	0.27	20.0	1	189	0.60
		2.58	0.05	4.5		17.4	17	38d					
VTU018	2009 BY86	2.11	0.24	2.0	0.60	17.7	4	1d	0.33	20.3	1	189	0.75
		2.32	0.15	1.0		18.8	16	18d					
VTU030	2009 FS67	2.39	0.12	5.1	1.11	18.0	5	1d	0.23	20.2	3	202	0.52
		2.76	0.09	7.7		16.5	26	10y					
VTU033	2009 FK20	2.36	0.29	3.8	0.67	18.8	5	1d	0.41	20.2	8	208	0.43
		2.65	0.28	4.9		17.2	22	35d					
VTU035	2002 GU116	2.24	0.04	7.1	1.14	17.1	5	1d	0.19	19.6	8	208	0.50
		2.33	0.17	7.3		17.4	49	9y					
VTU038	215040	2.45	0.05	6.9	1.35	15.6	5	1d	0.20	19.1	10	232	0.16
		2.55	0.13	7.2		16.0	52	7y					



Table A.7: Outstanding unknown objects observed at the INT.

Acronym	$a$	$e$	$i$	MOID	$H$	pos	arc	$rms$	$R$	$\beta$	$\epsilon$	$\mu$
VBA001	2.26	0.13	5.6	0.98	18.2	5	1d	0.23	20.2	8	208	0.45
VBA002	2.72	0.23	11.0	1.11	18.4	5	1d	0.22	20.8	8	208	0.51
VBA003	1.80	0.02	23.5	0.79	19.0	5	1d	0.08	21.1	43	219	0.45
VBA004	2.66	0.30	11.7	0.90	17.4	3	1d	0.53	20.2	-9	165	0.67
VBA005	2.65	0.31	4.7	0.85	17.8	5	1d	0.85	20.2	-8	165	0.68
VBA006	2.27	0.22	4.6	0.77	18.7	5	1d	0.26	19.7	-8	165	0.47
VDT055	2.61	0.00	2.3	1.60	17.4	5	1d	0.24	20.6	-1	167	0.57
VDT056	2.38	0.11	6.0	1.12	18.7	3	1d	0.17	20.8	-1	167	0.62
VDT057	2.24	0.24	5.4	0.71	19.2	4	1d	0.44	20.6	-1	167	0.71
VDT058	2.44	0.21	0.7	0.93	19.1	4	1d	0.31	20.6	-1	167	0.53
VDT071	2.28	0.40	5.0	0.39	19.0	4	1d	0.43	19.8	10	151	0.51
VIBC01	2.32	0.07	5.1	1.15	16.6	5	1d	0.08	20.1	-1	137	0.26
VIBC02	2.54	0.50	2.5	0.28	18.9	5	1d	0.07	19.9	-1	137	0.38
VIBC03	2.41	0.47	4.9	0.29	19.6	5	1d	0.09	20.0	-1	137	0.39
VIBC04	2.48	0.06	3.7	1.35	16.5	5	1d	0.13	19.8	-1	137	0.19
VIT001	2.52	0.24	8.3	0.93	17.5	4	1d	0.28	20.2	4	240	0.50
VIT002	1.97	0.02	23.9	0.92	17.5	4	1d	0.54	20.2	4	240	0.54
VIT004	2.33	0.32	1.0	0.57	16.2	5	1d	0.13	20.4	-1	137	0.35
VIT006	2.24	0.19	5.9	0.80	18.6	4	1d	0.25	20.8	-9	167	0.69
VITB01	3.28	0.01	21.1	2.25	14.5	5	1d	0.26	20.1	-9	92	0.43
VTD005	2.20	0.30	5.3	0.56	19.4	3	1d	0.44	19.4	14	179	0.46
VTD006	2.25	0.32	5.4	0.56	19.7	3	1d	0.16	19.6	14	179	0.44
VTD007	2.99	0.02	10.7	1.94	15.5	3	1d	0.43	19.4	15	179	0.55
VTD008	2.34	0.10	5.9	1.13	18.3	4	1d	0.41	20.8	11	152	0.40
VTD009	2.22	0.31	1.0	0.55	20.6	5	1d	0.27	20.1	0	178	0.44
VTD010	2.63	0.26	21.3	0.97	19.0	5	1d	0.30	20.2	0	178	1.02
VTD011	3.08	0.05	2.9	1.93	16.8	5	1d	0.24	20.4	0	178	0.54
VTD013	2.37	0.08	0.5	1.19	18.1	5	1d	0.19	20.0	0	177	0.67
VTD014	2.46	0.22	3.1	0.93	19.0	5	1d	0.26	20.1	0	177	0.60
VTD015	2.35	0.30	1.2	0.65	20.1	5	1d	0.22	20.1	0	178	0.49
VTD016	2.21	0.10	4.5	1.00	18.1	5	1d	0.16	19.4	0	178	0.69
VTD017	2.37	0.25	2.4	0.78	19.5	5	1d	0.80	20.1	0	177	0.57
VTD018	2.30	0.02	6.2	1.25	17.9	5	1d	0.43	20.2	0	177	0.70
VTD019	2.06	0.34	4.7	0.35	16.7	5	1d	0.35	20.0	0	177	0.70
VTD021	2.01	0.02	5.6	0.99	18.5	5	1d	0.64	19.9	0	177	0.74
VTD022	2.28	0.31	3.6	0.58	20.0	4	1d	0.81	19.6	0	178	0.54
VTD026	2.28	0.08	6.9	1.08	16.8	5	1d	0.41	19.4	0	178	0.71
VTD028	2.14	0.12	2.7	0.89	19.3	5	1d	0.55	20.3	0	178	0.69
VTD029	2.40	0.20	3.3	0.93	19.2	5	1d	0.45	20.3	0	178	0.63
VTD032	2.34	0.17	3.3	0.96	19.2	5	1d	0.39	20.4	0	178	0.65
VTD033	2.78	0.15	9.8	1.38	17.6	4	1d	0.26	20.0	0	178	0.62
VTD034	3.06	0.17	2.7	1.53	17.7	4	1d	0.60	20.5	0	177	0.50
VTD035	2.38	0.22	7.7	0.86	18.3	5	1d	0.29	20.5	10	152	0.35
VTD036	2.29	0.06	6.3	1.18	17.5	5	1d	0.22	20.1	10	152	0.45
VTD037	2.37	0.06	6.4	1.23	17.4	5	1d	0.17	20.4	10	152	0.43
VTD038	2.24	0.14	5.5	0.94	18.9	4	1d	0.25	20.8	11	153	0.39
VTD039	2.21	0.38	4.7	0.40	19.8	4	1d	0.29	20.2	11	152	0.49
VTD043	2.56	0.02	19.9	1.51	16.3	4	1d	0.65	20.2	17	137	0.49
VTD044	3.17	0.18	17.4	1.63	16.1	4	1d	0.78	20.0	17	137	0.16
VTD045	2.37	0.02	3.4	1.34	17.9	5	1d	0.35	20.5	-1	167	0.61
VTD046	2.42	0.27	3.5	0.78	19.6	4	1d	0.31	20.5	-1	166	0.49

Table A.7 (continued) – Outstanding unknown objects observed at the INT.

Acronym	$a$	$e$	$i$	MOID	$H$	pos	arc	$rms$	$R$	$\beta$	$\epsilon$	$\mu$
VTD047	2.45	0.09	3.0	1.22	17.6	4	1d	0.61	19.9	-1	166	0.55
VTD049	2.31	0.21	3.5	0.83	18.9	5	1d	0.12	20.1	-1	166	0.57
VTD051	3.03	0.03	8.1	1.97	16.5	5	1d	0.52	20.5	-1	166	0.52
VTD052	2.39	0.17	0.8	0.99	18.8	5	1d	0.31	20.5	-1	166	0.57
VTD053	3.06	0.23	2.3	1.36	15.1	5	1d	0.30	20.2	-1	166	0.48
VTD054	3.06	0.05	3.6	1.92	16.1	4	1d	0.36	19.9	-1	166	0.50
VTD055	2.61	0.00	2.3	1.60	17.4	5	1d	0.24	20.6	-1	167	0.57
VTD056	2.38	0.11	6.0	1.12	18.7	3	1d	0.17	20.8	-1	167	0.62
VTD057	2.24	0.24	5.4	0.71	19.2	4	1d	0.44	20.6	-1	167	0.71
VTD058	2.44	0.21	0.7	0.93	19.1	4	1d	0.31	20.6	-1	167	0.53
VTD059	2.57	0.12	6.9	1.25	17.0	4	1d	0.36	20.4	10	151	0.40
VTD060	2.66	0.46	4.7	0.46	18.9	5	1d	1.04	20.3	10	151	0.45
VTD061	2.51	0.31	9.2	0.77	16.7	5	1d	0.90	20.1	10	151	0.45
VTD062	2.23	0.17	6.3	0.87	17.1	5	1d	0.46	20.7	10	151	0.49
VTD063	2.03	0.16	4.8	0.72	19.4	5	1d	0.30	20.7	10	151	0.38
VTD064	3.11	0.51	4.8	0.53	19.3	5	1d	0.56	21.0	10	151	0.44
VTD066	2.31	0.20	7.2	0.85	19.3	4	1d	0.28	21.1	10	151	0.47
VTD069	3.01	0.52	10.2	0.51	19.4	4	1d	0.51	20.5	10	151	0.60
VTD070	2.35	0.18	2.2	0.93	19.7	7	1d	0.50	21.3	0	162	0.50
VTD071	2.44	0.17	7.4	1.01	17.5	6	1d	1.27	21.2	0	162	0.58
VTD072	2.51	0.35	3.9	0.66	19.7	7	1d	0.80	21.4	0	162	0.64
VTU004	2.49	0.06	11.3	1.35	16.2	5	1d	0.47	20.3	-13	102	0.52
VTU005	2.40	0.14	2.6	1.07	18.4	7	1d	0.17	20.0	4	183	0.63
VTU007	2.31	0.23	4.1	0.79	18.1	8	1d	0.11	18.9	4	183	0.63
VTU009	2.34	0.20	3.4	0.89	19.0	4	1d	0.62	20.2	1	189	0.71
VTU011	2.27	0.03	6.6	1.20	17.4	6	1d	0.32	19.8	6	182	0.70
VTU012	2.69	0.12	6.6	1.39	17.6	3	1d	0.17	20.2	7	182	0.60
VTU014	2.38	0.29	2.8	0.69	19.8	5	1d	0.38	20.2	7	183	0.51
VTU016	2.57	0.01	2.4	1.53	16.8	5	1d	0.21	19.9	1	189	0.60
VTU019	2.54	0.05	7.6	1.41	16.7	3	1d	0.20	19.9	7	183	0.63
VTU020	1.84	0.14	22.0	0.58	18.3	6	1d	0.31	20.3	41	229	0.67
VTU021	1.03	0.02	2.1	0.02	26.4	3	1d	0.43	18.9	-9	173	4.61
VTU022	2.43	0.07	2.1	1.27	17.1	4	1d	0.43	20.5	3	202	0.52
VTU023	2.31	0.23	1.2	0.77	19.5	4	1d	0.19	20.6	3	202	0.39
VTU024	2.47	0.16	1.9	1.09	16.9	4	1d	0.23	20.6	3	202	0.50
VTU025	2.41	0.03	2.5	1.33	17.8	3	1d	0.19	20.6	3	202	0.51
VTU026	2.36	0.01	2.8	1.33	17.9	4	1d	0.24	20.7	3	202	0.52
VTU027	2.43	0.16	9.9	1.03	18.5	4	1d	0.44	20.6	3	202	0.56
VTU028	2.39	0.46	7.2	0.30	17.4	3	1d	0.26	20.6	3	202	0.72
VTU029	2.20	0.15	3.5	0.86	18.9	5	1d	0.46	20.5	3	202	0.59
VTU031	1.99	0.03	19.6	0.92	18.8	5	1d	0.14	20.5	3	202	0.90
VTU032	2.30	0.16	4.6	0.93	18.8	4	1d	0.38	20.7	8	208	0.40
VTU034	2.26	0.07	4.9	1.12	18.3	3	1d	0.12	20.7	8	208	0.43
VTU036	2.62	0.16	6.1	1.22	18.2	5	1d	0.54	20.9	8	208	0.33
VTU037	2.99	0.03	11.2	1.93	16.2	5	1d	0.22	20.1	16	187	0.53

# EURONEAR - Recovery, Follow-up and Discovery of NEAs and MBAs using Large Field 1-2m Telescopes<sup>☆</sup>

O. Vaduvescu<sup>a,b,c,d,\*</sup>, M. Birlan<sup>b,e</sup>, A. Tudorica<sup>f,g,h,i</sup>, A. Sonka<sup>j,k</sup>, F. Pozo N.<sup>c</sup>, A. Barr D.<sup>c</sup>,  
D. J. Asher<sup>l</sup>, J. Licandro<sup>d,m</sup>, J. L. Ortiz<sup>n</sup>, E. Unda-Sanzana<sup>c</sup>, M. Popescu<sup>b,k,o</sup>, A. Nedelcu<sup>b,e</sup>,  
D. Dumitru<sup>h,k</sup>, R. Toma<sup>g,h,p</sup>, I. Comsa<sup>q</sup>, C. Vancea<sup>h</sup>, D. Vidican<sup>k</sup>, C. Opriseanu<sup>k</sup>, T. Badescu<sup>h</sup>,  
M. Badea<sup>h</sup>, M. Constantinescu<sup>k</sup>

<sup>a</sup>Isaac Newton Group of Telescopes (ING), Apartado de Correos 321, E-38700 Santa Cruz de la Palma, Canary Islands, Spain

<sup>b</sup>IMCCE, Observatoire de Paris, 77 Avenue Denfert-Rochereau, 75014 Paris Cedex, France

<sup>c</sup>Instituto de Astronomía, Universidad Católica del Norte (IA/UCN), Avenida Angamos 0610, Antofagasta, Chile

<sup>d</sup>Instituto de Astrofísica de Canarias (IAC), C/Vía Láctea s/n, 38205 La Laguna, Spain

<sup>e</sup>Astronomical Institute of the Romanian Academy, Căminul de Argint 5, Bucharest 040557, Romania

<sup>f</sup>Bonn Cologne Graduate School of Physics and Astronomy, Germany

<sup>g</sup>Argelander-Institut für Astronomie, Universität Bonn, Auf dem Hügel 71 D-53121 Bonn, Germany

<sup>h</sup>University of Bucharest, Department of Physics, CP Mg-11, Bucharest Magurele 76900, Romania

<sup>i</sup>Institute for Space Sciences, Bucharest - Magurele, Ro-077125 Romania

<sup>j</sup>Astronomical Observatory "Admiral Vasile Urseanu", B-dul Lascar Catargiu 21, Bucharest, Romania

<sup>k</sup>Bucharest Astroclub, B-dul Lascar Catargiu 21, sect 1, Bucharest, Romania

<sup>l</sup>Armagh Observatory, College Hill, Armagh BT61 9DG, UK

<sup>m</sup>Departamento de Astrofísica, Universidad de La Laguna, E-38205 La Laguna, Tenerife, Spain

<sup>n</sup>Instituto de Astrofísica de Andalucía (IAA), CSIC, Apt 3004, 18080 Granada, Spain

<sup>o</sup>Polytechnic University of Bucharest, Faculty of Applied Sciences, Department of Physics, Bucharest, Romania

<sup>p</sup>Romanian Society for Meteors and Astronomy (SARM), CP 14 OP 1, 130170, Targoviste, Romania

<sup>q</sup>Babes-Bolyai University, Faculty of Mathematics and Informatics, 400084 Cluj-Napoca, Romania

## Abstract

We report on the follow-up and recovery of 100 program NEAs, PHAs and VIs using the ESO/MPG 2.2m, Swope 1m and INT 2.5m telescopes equipped with large field cameras. The 127 fields observed during 11 nights covered 29 square degrees. Using these data, we present the incidental survey work which includes 558 known MBAs and 628 unknown moving objects mostly consistent with MBAs from which 58 objects became official discoveries. We planned the runs using six criteria and four servers which focus mostly on faint and poorly observed objects in need of confirmation, follow-up and recovery. We followed 62 faint NEAs within one month after discovery and we recovered 10 faint NEAs having big uncertainties at their second or later opposition. Using the INT we eliminated 4 PHA candidates and VIs. We observed in total 1,286 moving objects and we reported more than 10,000 positions. All data were reduced by the members of our network in a team effort, and reported promptly to the MPC. The positions of the program NEAs were published in 27 MPC and MPEC references and used to improve their orbits. The O-C residuals for known MBAs and program NEAs are smallest for the ESO/MPG and Swope and about four times larger for the INT whose field is more distorted. For the astrometric reduction, the UCAC-2 catalog is recommended instead of USNO-B1. The incidental survey allowed us to study statistics of the MBA and NEA populations observable today with 1–2m facilities. We calculate preliminary orbits for all unknown objects, classifying them as official discoveries, later identifications and unknown outstanding objects. The orbital elements  $a$ ,  $e$ ,  $i$  calculated by FIND\_ORB software for the official discoveries and later identified objects are very similar with the published elements which take into account longer observational arcs; thus preliminary orbits were used in statistics for the whole unknown dataset. We present a basic model which can be used to distinguish between MBAs and potential NEAs in any sky survey. Based on three evaluation methods, most of our unknown objects are consistent with MBAs, while up to 16 unknown objects could represent NEO candidates and four represent our best NEO candidates. We assessed the observability of the unknown MBA and NEA populations using 1m and 2m surveys. Employing a 1m facility, one can observe

today fewer unknown objects than known MBAs and very few new NEOs. Using a 2m facility, a slightly larger number of unknown than known asteroids could be detected in the main belt. Between 0.1 and 0.8 new NEO candidates per square degree could be discovered using a 2m telescope.

**Keywords:** minor planets, near Earth asteroids, main belt asteroids, orbits, astrometry, follow-up, survey, discovery

---

## 1. Introduction

Near Earth Asteroids (NEAs) are defined as minor planets with a perihelion distance  $q \leq 1.3$  AU and an aphelion distance  $Q \geq 0.983$  AU (Morbidelli et al., 2002). Potentially Hazardous Asteroids (PHAs) are NEAs having a minimum orbital intersection distance  $MOID \leq 0.05$  AU and an absolute magnitude  $H \leq 22$  mag (Bowell and Muinonen, 1994). Virtual Impactors (VIs) represent objects for which the future Earth impact probability is non-zero according to the actual orbital uncertainty (Milani and Gronchi, 2009).

According to present data (e.g. Bowell, 2011), there are more than half a million orbits of known Main Belt Asteroids (MBAs) and about 7,600 catalogued NEAs of which about 1,200 are PHAs (NASA, 2011) and ca 100 VIs (NEODyS, 2011). During the last two decades the total numbers of discovered NEAs and PHAs have continued to grow, mainly thanks to five dedicated surveys led by the United States (CSS, LINEAR, Spacewatch, LONEOS and NEAT) which have been using large field mostly 1m class telescopes. Together, they have discovered 86.8% of the entire NEA population known today (MPC Jan 2011 database), while Europe accounts for less than 1% (led by La Sagra and Crni Vrh mostly run by amateurs). Some European initiatives were taken by national institutions or local collaborations (ASIAGO/ADAS in Italy and Germany, CINEOS in Italy, KLENOT in the Czech Republic, NEON in Finland) and a few programs to study physical properties of NEAs have been carried out by groups in Europe (led by P. Pravec in the Czech Republic, SINEO led by M. Lazzarin in Italy, another program led by J. Licandro in Spain, etc). Thus although there is still no common European program and no dedicated telescope to observe NEAs, the existence of this expertise, in addition to extensive observational facilities, evidently provides an opportunity for Europe to improve its number of discoveries.

In spite of the larger facilities apparently available today, extremely few researchers have used 2m class or larger facilities to observe fainter NEAs. During two short runs at ESO La Silla, Boattini et al. (2004) employed the ESO/MPG 2.2m as a search facility and the NTT 3.5m as a follow-up telescope to survey faint NEAs and MBAs beyond 22nd magnitude. During three nights using the ESO/MPG facility, the authors incidentally observed about 700 MBAs as faint as  $R = 21.5$  mag ( $V \sim 22$  mag) exposing between 60 and 150 sec in the  $R$  band. Using only four hours in override service mode at the Yepun VLT 8.2m telescope, Boattini et al. (2003) eliminated 4 very faint VIs ( $22 < V < 25$  mag), shifting them to simply the NEA or PHA class.

Although the known NEA and PHA populations have increased during the last few decades, the annual growth of the number of known NEAs and PHAs appears to be becoming constant during recent years (EARN, 2011), probing some size threshold due to the limiting magnitude

---

<sup>☆</sup>Based on observations taken with the telescopes ESO/MPG 2.2m in La Silla (ESO Run number 080.C-2003), Swope 1m in Las Campanas (CNTAC 2008) and the INT 2.5m in La Palma (CAT DDT 2010).

\*Corresponding author

Email address: ovidiu@ing.iac.es (O. Vaduvescu)

$V \sim 21$  mag reached by the present 1m class surveys. It is unclear whether new 2m surveys such as the Spacewatch 1.8m and especially the new Pan-STARRS PS1 1.8m (although not entirely dedicated to NEAs) will make a significant contribution to the completeness of NEAs through the small size objects.

During the last four years, the European Near Earth Asteroids Research (EURONEAR) program has observed to date 234 program NEAs, defined as NEAs specifically planned to be observed according to a few selection criteria to be discussed below. Throughout our program, we used 10 mostly 1m class telescopes, in visiting mode, contributing with follow-up astrometry and recovery of some important NEAs, PHAs and VIs, allowing their orbits to be secured or improved (Birlan et al., 2010). Part of this work, three telescopes in Chile and the Canaries, represent our largest facilities employed, namely the ESO/MPG 2.2m in La Silla, Swope 1m in Las Campanas, and the INT 2.5m in La Palma, all equipped with large field cameras. To take advantage of these facilities, incidentally to our main program NEA work, we have identified many known MBAs in the observed fields and have also discovered many new objects.

In this paper we review our EURONEAR observations at ESO/MPG and Swope and we present our new observations at the INT. Besides presenting our main NEA follow-up program, we introduce and discuss our incidental survey work using the observed fields, classifying all the observed sources as known MBAs, unknown MBAs and NEA candidates. By comparing the statistics obtained from our survey on the three 1–2m facilities, and also with those obtained from other authors using 4m and 8m telescopes, we assess the observability limits of the MBA and NEA populations observable with 1m and 2m telescopes. In Section 2 of the paper we explain the basic principles driving the planning, observations and data reduction of our runs. In Section 3 we present the results, including program NEAs, known MBAs and other unknown objects. In Section 4 we discuss the results, focusing on the known and unknown MBA and NEA populations, comparing all three facilities and presenting some statistics. The conclusions are presented in Section 5.

## 2. Observations and Data Reduction

As part of the EURONEAR project, between 2008 and 2010 we obtained three runs and a total of 11 nights for proposals devoted to the recovery and follow-up of some important NEAs, PHAs and VIs using the ESO/MPG and Swope telescopes in Chile and the INT in La Palma. For each run, the targets were selected based on the daily updated known NEA population.

### 2.1. Planning the Runs

To search and prioritize the objects, we have used four planning servers with which one can check on a daily or hourly basis the updated NEA database. To complement the existing surveys focused on discovery, we focused our EURONEAR runs on some important objects in need of orbital improvement, especially on newly discovered faint asteroids which need to be secured against loss and also on other older objects having a short observed arc which needs to be improved at the second or a later opposition. We selected our targets taking into account the following six *criteria*:

1. Object class: observe objects classified as VIs, PHAs or NEAs (in this order), to improve their orbits and confirm or change their classification;
2. Time interval from discovery: secure and follow-up poorly observed objects, a few days or weeks from discovery;

3. Number of oppositions: recover objects previously observed at very few oppositions (especially one-opposition objects);
4. Object brightness: recover and follow-up faint and very faint objects, accessible only to larger facilities (larger than 2m) in danger of being lost by current surveys;
5. Positional uncertainty: recover and follow-up poorly observed objects having large positional uncertainty (up to one degree), less accessible to other smaller field facilities;
6. New object confirmation: recover newly discovered objects, preferably a few to several hours after their discovery;

To implement these criteria, we have used the following four *planning servers*:

1. EURONEAR Planner 1: queries the Spaceguard database for mostly newly discovered objects;
2. EURONEAR Planner 2: queries the MPC Bright and Faint Recovery Opportunity databases for mostly older objects in need of being recovered at a new opposition;
3. MPC NEO Confirmation Page: includes 1-night objects in need of being confirmed by independent observers;
4. NASA/JPL Close Approaches List: includes closest approaches of old and new objects visible from Earth;

Both EURONEAR planner web-services are accessible online (EURONEAR, 2011), being written in PHP by our team and offered to the community for planning other NEA follow-up campaigns. The servers query the current Spaceguard or MPC databases (both updated on a daily basis) and return the prioritized observing lists given the observing place, facility and observing date. The planning is based on eight calculated observability factors, namely: the asteroid class (according to MPC), the apparent magnitude, proper motion, ephemeris uncertainty, altitude, star density in the field, and Moon illumination and distance, calculated with a time step (e.g., one hour) in a given time interval (e.g., one night). The result consists of a few tables listing at each step the recommended observable objects prioritized according to the object apparent magnitude, its altitude (or airmass), proper motion, sky plane error, or some proposed “Observability” factor calculated as the product of all the above individual observability factors. Two accurate ephemeris servers, namely NEODyS (NEODyS, 2011) and IMCCE (IMCCE, 2011), are queried by the planning server automatically, returning sky coordinates, magnitudes and uncertainties according to the observed orbital arc. The response time for both servers is short, usually less than one minute for one night’s information.

## 2.2. Observations

We present here our observing runs at ESO/MPG in La Silla, Swope in Las Campanas and INT in La Palma.

### 2.2.1. ESO/MPG Observing Run

During 3 nights from 10–13 Mar 2008 we used the ESO/MPG 2.2m telescope at ESO La Silla, Chile to observe 15 program NEAs, PHAs and VIs. At the Cassegrain  $F/5.9$  focus of the telescope we used the Wide Field Imager (WFI) which consists of a  $2 \times 4$  mosaic of CCDs  $2K \times 4K$  pixels each, covering a total field of view of  $34' \times 33'$  with a pixel scale of  $0.24''/\text{pix}$ .

Due to the relatively high proper motion of NEAs at opposition (around  $2 - 3''/\text{min}$ ), the average seeing of about  $1 - 1.5''$ , and taking into account the large raw image size on disk (140

MB) combined with the relatively slow readout time compared with our fast planned cadence, we observed the entire run in binning mode  $3 \times 3$  ( $0.71''$  pixel size). We used an  $R$  band filter for the entire run. This binning does not affect the quality of our astrometry (set by the goal of having astrometric errors less than  $0.3''$ , i.e., comparable with the star catalog reference), as can be observed from the statistics in Section 3.

To take advantage of the large MPG and WFI facility, we focused our run on two aspects, namely to follow-up some important NEAs, and to discover and recover many MBAs appearing in the observed fields. The weather was clear all three nights, with only two hours lost due to high humidity at the beginning of the first night. The sky was dark, with the Moon 3–6 days past new.

In Table A.1. of our past paper (Birlan et al., 2010) we listed the 15 observed NEAs during our ESO/MPG run, 6 VIs, 4 PHAs and 5 other NEAs. Besides the 15 NEA program fields, during the following available nights we observed nine neighbouring fields, in order to secure some MBAs discovered in the previous nights. The neighbouring fields were chosen assuming a proper motion of  $0.7''/\text{min}$  for MBAs observed near opposition. During the second night only, we also surveyed 8 WFI fields (2.5 square degrees) in the ecliptic, about  $50^\circ$  from opposition to avoid crowding from the Milky Way. Besides the program NEAs, we identified and measured all moving sources in all the observed fields, reporting all known and new objects visible up to  $V \sim 22$  mag. During all three nights at ESO/MPG, we observed in total 42 WFI fields covering about 13 square degrees.

#### 2.2.2. Swope Observing Run

During 5 nights on 18–19 Oct and 22–24 Oct 2008 we used the Swope 1m telescope in Las Campanas Observatory (LCO), Chile, to observe 50 program NEAs. At the Cassegrain  $F/7$  focus of the telescope we used the *SITe#3*  $2K \times 3.6K$  pixel camera giving a field of  $15.1' \times 26.5'$  with a pixel scale  $0.43''/\text{pix}$ . We used an  $R$  band filter and no binning for the entire run. The sky was gray (Moon up to 4 days from last quarter) and the weather was very good, with seeing around  $1''$ .

In Table A.1. of our past paper (Birlan et al., 2010) we listed our 50 observed NEAs during the Swope run, 12 PHAs and 38 other NEAs. Besides the program NEAs, we identified and measured all moving sources in the observed fields, reporting all known and new objects visible up to  $R \leq 20.4$  mag. During five nights we observed in total 50 Swope fields covering some 6 square degrees.

#### 2.2.3. INT Observing Runs

During two discretionary nights (D-nights) on 12 Feb and 15 Apr 2009 (3+3 hours), one hour in 13/14 Nov 2009 and 4 nights awarded by the Spanish Director's Discretionary Time (DDT) in 20–25 Feb and 3 Mar 2010, we used the INT 2.5m telescope in Roque de Los Muchachos Observatory (ORM) in La Palma to observe 35 program NEAs, namely 1 VI, 13 PHAs and 21 other NEAs. At the prime focus of the INT we used the Wide Field Camera (WFC) which consists of 4 CCDs  $2K \times 4K$  pixels each, covering an L-shape  $34' \times 34'$  with a pixel scale of  $0.33''/\text{pix}$ . Both D-nights and 13/14 Nov 2009 were observed without binning, while the Feb-Mar 2010 run was observed with  $2 \times 2$  binning ( $0.66''/\text{pix}$ ) to minimize the readout time and match the poor weather conditions. We used an  $R$  filter for all runs.

Most of the INT time was bright and gray, with only three hours dark time. The weather was good during the first 6 hours on the first two D-nights and one hour in 13/14 Nov 2009, but very bad (wet and windy) during the whole DDT run (Feb-Mar 2010) when the Moon was

gray and bright. In Table 1 we list the INT program NEAs, including the object classification, proper motion,  $3\sigma$  positional uncertainty (according to the MPC for the observing date) and the orbital arc length at the observing date. Besides the program NEAs, at the INT we identified and measured all moving sources in all observed fields, reporting all known and new objects visible up to  $R \sim 21.2$  mag. In total at the INT, we observed for about three clear nights, a total of 35 WFC fields covering some 10 square degrees.

### 2.3. Data Reduction

For all runs, we processed the data within 2–3 days from observations using an IRAF pipeline (for the INT and Swope data) and IDL (for ESO/MPG data), taking into account the usual subtraction of the appropriate bias and sky flat field. For the WFI and WFC mosaic cameras we sliced CCD images and treated them independently, calculating CCD centres based on the pointing of the telescope (included in the image headers) and the geometry of the two cameras. All images were processed on-site, then archived and eventually transferred via FTP to the remote available data reducers, allocated on demand.

In order to secure some unknown objects, we observed at ESO/MPG nine fields in multiple nights, seven imaged during two nights and two fields during three nights. To identify objects observed in multiple nights, we extrapolated in time the arcs of all moving sources observed during the first night using a least square fitting code written by our team. By comparing the extrapolated positions of objects observed in one field during the first night for the observing date corresponding to the second night with the positions of the objects observed in the follow-up field during the second night, one could easily pair objects in the  $\alpha - \delta$  position space. In case of crowding and close matches, the magnitude represents a second indicator. Using this pairing technique we matched all the unknown objects observed during multiple nights, namely 43 objects observed during two nights and 8 objects observed during 3 nights. Thanks to this confirmation, most of these objects became credited discoveries. Figure 1 presents an example of such identification of objects observed in a crowded field ( $9^\circ$  from opposition and  $4^\circ$  south of the ecliptic). With cyan circles we plot predicted positions and with magenta circles observed positions.

The reduced images were analysed and measured using Astrometrica (Raab, 2011), carefully visually blinking all images of the same field in order to detect all moving objects. Around 100 reference stars (UCAC-2 for Swope data or USNO-B1 for ESO/MPG and INT data) were used for each CCD to perform the astrometry, using a linear model in the cases of WFI and Swope known to have small field distortion and fitting a 3-degree polynomial in the case of WFC to accommodate its larger optical field distortion. According to the literature and also to our derived astrometry (Section 3.1), the astrometric errors due to the field distortion appear very small for the WFI field, being mostly within  $0.1''$  across most of the WFI field (about 90%), according to the field distortion pattern derived by Assafin et al (2010) which shows the largest distortion in the corners of the mosaic (up to  $0.53''$ ) and some distortion around  $0.2''$  in the upper and lower edge and the centre of the mosaic. Relative photometry was derived by Astrometrica using from a dozen to a few hundred catalog stars visible in the field, the reduced asteroid magnitudes having an uncertainty of about 0.1 mag. For all runs, we decided to use Astrometrica in preference to other software because of its simplicity, common platform and simple installation and usage by all members of the team, as many of the data reducers were students and amateurs. We inspected the data visually instead of using automated software, because of the relatively low volume of data per run, and mostly because the human eye and brain are known to detect faint moving



sources better than the computer. We detected asteroids as low as ca  $1.5\sigma$  level from noise, which allowed us to recover many faint targets inaccessible to other automated surveys.

All the reduced data (output of Astrometrica in MPC format) were collected by the PI of the run, checked for errors using the EURONEAR O–C calculator or the FITSBLINK residual calculator (Skvarc, 2010a), then submitted to the MPC in three groups: the observed NEAs, the known asteroids, and the unknown asteroids (possibly discovered by us).

### 3. Results

During all three runs, we observed effectively in total about 11 nights, reporting positions and magnitudes for 100 program NEAs (7 VIs, 29 PHAs and 64 NEAs), 558 known MBAs and 628 unknown moving objects, in total 1286 objects observed in 29 square degrees total surveyed field.

Table 2 presents the overview of our observations at ESO/MPG, Swope and INT, listing the number of observed objects, number of reported positions and the standard deviation of the orbital fit using our data (according to NEODyS). We classify the objects in three groups: observed NEAs, known MBAs, and the unknown (unidentified) objects. We further classify the unknown objects in three groups: official discoveries, later identifications and outstanding objects. We include the number of nights observed at each facility, the number of observed fields, the total sky coverage (in square degrees) and the limiting magnitude for each facility. Next, we give the total number of objects. Finally, we conclude with some density statistics which will be discussed in Section 4.4.

#### 3.1. Program NEAs

In the left panels of Figures 2, 3 and 4 we plot the O–C residuals (observed minus calculated) in  $\alpha$  and  $\delta$  for the program NEAs observed at ESO/MPG, Swope and INT, based on the orbital fits available on 22 Nov 2010 (NEODyS, 2011). The O–C standard deviations are  $0.15''$  for the ESO/MPG dataset,  $0.39''$  for Swope and  $0.42''$  for the INT.

In total, 27 MPC and MPEC publications include data from our three runs. Table 3 includes these references: 12 publications containing our Swope observations, 10 our ESO/MPG observations and 6 publications including our INT data.

Birlan et al. (2010) presented the most important NEAs recovered at ESO/MPG and Swope. At ESO/MPG we observed 12 faint objects (6 VIs, 3 PHAs and 3 NEAs) less than one month after discovery, and also recovered 2 faint objects (1 PHA and 1 NEA) at their second or later opposition. With Swope we observed 25 objects (all NEAs) soon after discovery, recovering also 2 objects (one NEA and one PHA) at their second or later opposition. From Table 1 we can count the number of recoveries using the INT: 25 objects soon after discovery (1 VI, 8 PHAs and 16 NEAs) and 6 faint objects having large uncertainty recovered at their second or later opposition (2 PHAs and 4 NEAs).

Nine especially important NEAs were observed with the INT. We mark them with \* in the first column of Table 1 and we discuss them next. Thanks to the the large aperture of the INT and the large field of the WFC, we eliminated 3 NEA candidates and 1 VI. First classified as a NEA, 2009 CB2 had a poor orbit (2 day arc) and a very high sky uncertainty ( $3\sigma = 1000''$ ). Thanks to the large field of WFC, we recovered this object one week later, allowing its orbit to be improved and eliminating it from the NEA list. A similar case was 2010 CF12, originally classified as a NEA based on a small 3 day arc. Although the MPC did not list its sky uncertainty by the time

of our INT run, we recovered this object one week later and eliminated it from the NEA list. Another object degraded from the NEA class to the MBA class was 2010 DC. It had a small arc based on 4 nights data and a sky uncertainty of about  $1'$ , allowing fast recovery two weeks later at the INT. One of the most important detections of the INT was 2009 VR25, a new object classified as a VI based on its original poor two night orbit. Although quite faint ( $V = 20.7$  mag) and having very large sky uncertainty ( $3\sigma = 1400''$ ), we could find it, enabling its reclassification from the VI to NEA class.

We recovered 3 NEAs at their second opposition with the INT. 2007 RM133 was discovered in 2007, having a short arc (one month) at the time of the INT run. Despite its very faint magnitude ( $V = 21.4$  mag) and very large sky uncertainty ( $3\sigma = 490''$ ), we recovered it 3 years later, allowing a substantial improvement of its orbit (Holvorcem et al, 2010). Another second opposition recovery was 2003 SJ84, another NEA observed for only one month, following its discovery in 2003. Although very faint ( $V = 21.4$  mag) and having quite large positional uncertainty ( $3\sigma = 81''$ ), we recovered it six years later about  $21'$  away from its predicted position (15 times more than its nominal MPC  $3\sigma$  value) and we improved its orbit (Fitzsimmons et al., 2009). Our best ever second opposition recovery was 2000 SV20. This NEA was observed for 3 months following its discovery in 2000 and recovered 10 years later by the INT/WFC about  $7'$  away from its predicted MPC position (7 times more than the nominal MPC  $3\sigma \sim 1'$  value).

Using the INT, in 2010 we followed two Arecibo radar targets. 2010 DJ1 was requested by NASA in Feb 2010 (Benner, 2010), having an uncertainty ( $3\sigma = 190''$ ) which allowed its INT recovery only three days after discovery. 2007 EF was another Arecibo target, moving very fast ( $\mu = 20''/\text{min}$ ) but allowing successful WFC imaging at  $V = 18.2$  mag in only 10 sec exposures.

### 3.2. Known MBAs

During all three runs in the observed program NEA fields, we observed incidentally a total of 558 known MBAs.

In the right panels of Figures 2, 3 and 4 we plot the O–C residuals for the known MBAs observed in all three runs based on their current orbits available at 22 Nov 2010 (AstDyS, 2011). The standard deviations are  $0.15''$  for the ESO/MPG dataset,  $0.18''$  for Swope and  $0.66''$  for the INT.

The standard deviations of the ESO/MPG dataset for both NEAs and MBAs are very small, proving the excellent quality of this telescope equipped with the WFI which allowed very accurate astrometry across its whole large field. Nevertheless, a systematic offset to the north of  $0.111'' \pm 0.001''$  in  $\delta$  and  $0.037'' \pm 0.001''$  in  $\alpha$  shows up in the right panel of Figure 2 for the known MBA dataset observed at ESO/MPG, with the observed median position located northwest of the calculated ephemerides. This effect is consistent with results of Tholen et al. (2008a) who found a surprising systematic offset of the astrometry of the asteroid Apophis of about  $0.2''$  based on 200 observations reduced with the USNO-B1 catalog (which was also used by us to reduce our ESO/MPG data). By comparing USNO-B1 with ICRF, the authors determined for the USNO-B1 an average declination offset of  $+0.116''$ , in perfect agreement with our findings.

The standard deviation of the Swope datasets is  $0.39''$  for the NEA data and  $0.11''$  for the MBA data, and no sample shows any systematic offset with respect to the origin. We reduced Swope data with the UCAC-2 catalog, known to have better astrometry than USNO-B1. Both for Swope and ESO/MPG runs, the standard deviation for the MBA sample is smaller than that of the NEA sample probably because of the higher S/N due to brighter and slower moving MBA objects, compared with the fainter and faster moving program NEAs.

The INT/WFC shows relatively large residuals for both NEA and MBA samples (up to about 2'' and standard deviation 0.66'' as quoted above) and only for this facility the deviation of the MBA sample is larger than that of the program NEAs. Bad weather did not impede the astrometry for our INT run, catalog stars being quite bright in a 2m telescope resulting in good S/N and sub-arcsec stellar positions. The USNO-B1 catalog has an average astrometric accuracy of 0.2'', too small to explain the larger residuals of the INT astrometry.

The larger residuals for known MBAs than for program NEAs observed with INT/WFC can however be explained taking into account that MBAs were imaged across the entire WFC field which is heavily affected by the field distortion at the INT prime focus, compared with the central CCD#4 where most of the NEAs were observed and the WFC field has the smallest distortion. Given this, for any future INT/WFC work we plan to correct the image field before data reduction.

### 3.3. Unknown Objects

A total of 467 unknown moving objects were identified at ESO/MPG, 41 at Swope and 120 at the INT (Table 2). The observed proper motion for most objects was compatible with MBAs with a few exceptions discussed next.

Throughout our paper and in Table 2 we classify the unknown objects in three categories: *official discoveries* (confirmed by the MPC according to their DISCSTATUS monthly list), *later identifications* (unknown objects which could be linked with existing arcs) and *outstanding objects* (waiting for orbital links from independent observations, possibly to be credited to us later).

#### 3.3.1. Unknown MBAs

We include in the Appendix A (available only in the online version of our paper) seven tables listing all the unknown objects observed at ESO/MPG (Tables A.1, A.2 and A.3), Swope (Tables A.4 and A.5) and the INT (Tables A.6 and A.7). We give first the official discoveries, then later identifications and finally outstanding objects.

Table A.1 includes our official discovered asteroids at ESO/MPG. We give first the EURONEAR object acronym (based on the initials of the surname of the observers and reducers<sup>1</sup>), then the official designation (from the MPC), three main orbital parameters (semimajor axis  $a$ , eccentricity  $e$  and inclination  $i$ ), Earth minimum orbital intersection distance  $MOID$ , absolute magnitude  $H$ , number of observed positions, arc length (in days or years), rms of the O-C residuals for the orbital fit  $\sigma$ , observed apparent magnitude  $R$ , ecliptic latitude  $\beta$ , Solar elongation  $\epsilon$  (both in degrees) and apparent proper motion  $\mu$  (in ''/min). We distinguish directions east and west of opposition by letting  $\epsilon$  increase above 180° for fields to the east.

For each object we give in the first line the orbital elements fitted with the FIND\_ORB software (Gray, 2011a) based on our observations only and for the standard epoch  $MJD = 54520.0$ . On the second line we list the orbital elements taken from the MPC database (MPC, 2011) calculated by fitting all MPC available observations for an epoch close to the mid-point interval of those observations.

Table A.2 includes the unknown objects (at the date of the run) which were identified later (in Nov 2010) with known objects, based on the checks of the MPC database and the MPC automatically assigning designations. Our calculated orbits, presented again in the first line, are

---

<sup>1</sup>VB = Vaduvescu and Birlan; TU = Tudorica; SO = Sonka; OP = Opriseanu; VI = Vidican; TO = Toma; VA = Vancea.

based on the very short available arc (observations acquired in less than one hour), and so should be regarded with caution.

For both official discoveries and later identified objects, the orbital elements from the first line are very close to the official elements in the second line. Although most of our fits are based on very short arcs observed during 1–3 nights at ESO/MPG and only one night at Swope and INT, one can observe the success of the FIND\_ORB fit for most objects, especially for the  $a$ ,  $e$  and  $i$  parameters which will be used in statistics later. In particular, based on 116 paired orbits available from the three runs, we can compare FIND\_ORB versus MPC by calculating the median values of the differences in  $a$ ,  $e$ ,  $i$  and  $H$ , which are 0.20 AU, 0.06,  $1.05^\circ$  and 0.70 mag, respectively.

Table A.3 includes the remaining unknown objects observed at ESO/MPG which could not be identified according to the present MPC database (Nov 2010). For them we give only our calculated orbits, based on very short arcs observed only in one night. The exact elements should be regarded with caution but are usable for statistics in Section 4.

Table A.4 lists the later identified objects observed with the Swope telescope, while Table A.5 gives the outstanding unknown objects observed with Swope. Similarly, Tables A.6 and A.7 give the later identified objects and outstanding unknown objects observed at the INT.

According to the MPC (Jan 2011 DISCSTATUS), our ESO/MPG run produced 58 official discoveries. Most of the people involved in EURONEAR work on a voluntary basis and include students and amateur astronomers based in Romania. Indeed, the entire ESO/MPG team included people of Romanian origin who became the first Romanian discoverers of minor planets (Vaduvescu, 2009). Given these, in 22 December 2008 we proposed to the Working Group for Small Body Nomenclature (CSBN) of the International Astronomical Union (IAU) a list including 12 Romanian names. In Jan 2011 the first two of our discovered asteroids received numbers, namely (257005) = 2008 EW152 = VBTU207 (our acronym) and (263516) = 2008 EW144 = VBTU224, being eligible for naming.

### 3.3.2. NEO Candidates

In this section we will use three tools to check all our unknown objects for potential Near Earth Objects (NEOs). In Table 4 we include all NEO candidates derived from all three methods, marking in bold the best candidates. Besides the observed properties (quantities  $\mu$ ,  $\epsilon$ ,  $R$ , number of positions and O–C standard deviation), we include in this table the orbital parameters ( $a$ ,  $e$ ,  $i$ ) and data derived from the three methods (MOID in column 4, MPC score in column 10 and the Model in the last column).

For the first method we plot in Figure 5 the apparent proper motion  $\mu$  versus the Solar elongation  $\epsilon$  for all the unknown objects observed at ESO/MPG (red), Swope (green) and the INT (blue). Observed in a given field near opposition (close to  $\epsilon \sim 180^\circ$ ), MBAs are expected to show proper motions distributed in a small vertical “finger”-shaped region with proper motions between  $\mu \sim 0.3 - 0.7''/\text{min}$ , depending on their location in the main belt. Observed further away from opposition, MBAs should show smaller proper motions owing to the larger distance and velocity projection effect. Both  $\mu$  and  $\epsilon$  represent quantities measured directly from observations, not being affected by the uncertain orbits derived from the short arc. Therefore the  $\mu - \epsilon$  plot represents an important method to search a survey for fast moving objects including NEAs, PHAs and other NEOs.

Let us consider the very basic orbital model which assumes the (prograde) asteroid orbit circular and coplanar with the circular orbit of Earth, and the asteroid at least  $90^\circ$  away from the Sun. Following Kolena (1999) we express the asteroid proper motion as a function  $\epsilon$ . Let  $\Delta$  be the angle between the directions of Sun and asteroid as seen from Earth ( $\Delta$  is  $\epsilon$  or  $360^\circ - \epsilon$ , with

$0 < \Delta < 180^\circ$ ). Let  $v_E$  and  $v_a$  be the orbital velocities of Earth and asteroid,  $\phi$  the angle as seen from the asteroid between the direction of Earth and that of the asteroid's orbital motion, and  $E$  the difference  $180^\circ$  minus the angle (as seen from Earth) between the direction to the asteroid and the direction of Earth's orbital motion (so  $E = \Delta - 90^\circ$ ). Then the angular speed of the asteroid  $\omega$  as seen from Earth is the difference in the projected velocities perpendicular to the Earth–asteroid direction, divided by the Earth–asteroid distance:

$$\omega = \frac{v_a \sin \phi - v_E \sin E}{d} \quad (1)$$

From the sine law applied to the triangle Sun–Earth–asteroid:

$$\sin \phi = \sqrt{1 - \frac{a_E^2 \sin^2 \Delta}{a_a^2}} \quad (2)$$

The cosine rule applied to the same triangle, solving the resulting quadratic for  $d$ , gives:

$$d = a_E \cos \Delta + \sqrt{a_a^2 - a_E^2 \sin^2 \Delta} \quad (3)$$

where we dropped the minus solution because  $d$  should always be positive. Kepler's third law (assuming Earth and asteroid masses very small compared with Sun's mass) implies  $v_a = \sqrt{\frac{GM_S}{a_a}}$  and  $v_E = \sqrt{\frac{GM_S}{a_E}}$  where  $G = 6.673 \times 10^{-11} \text{ m}^3 \text{ kg}^{-1} \text{ s}^{-2}$  is the gravitational constant,  $M_S = 1.989 \times 10^{30} \text{ kg}$  the Sun's mass and  $a_E = 1.496 \times 10^{11} \text{ m}$  the Earth's semimajor axis.

Substituting all these terms in Equation 1, and since  $\sin E = -\cos \Delta$ , we obtain the following formula for the apparent angular speed of the asteroid as a function of  $\Delta$  and  $a_a$ :

$$\omega = \frac{\sqrt{\frac{GM_S}{a_a}} \sqrt{1 - \frac{a_E^2 \sin^2 \Delta}{a_a^2}} + \sqrt{\frac{GM_S}{a_E}} \cos \Delta}{a_E \cos \Delta + \sqrt{a_a^2 - a_E^2 \sin^2 \Delta}} \quad (4)$$

Finally, the proper motion of the asteroid  $\mu$  in arcsec per minute can be calculated from the angular speed  $\omega$  in radians per second:

$$\mu = \omega \times \frac{180 \times 3600}{\pi} \times 60 \quad (5)$$

We can use Equation 5 and the asteroid semimajor axis  $a_a$  as a model to map the expected limits for the proper motion of MBAs (defined between  $a_a = 2.0$  and  $a_a = 3.5 \text{ AU}$ ). In the context of this basic orbital model where we consider proper motions (as a function of elongation) only, we may also represent NEOs by considering orbits with  $a_a < 1.3 \text{ AU}$ . By plotting the values of  $\mu$  between solar elongations  $90^\circ$  and  $270^\circ$  (e.g., using one degree step in  $\epsilon$ ), one can draw the limits corresponding to these populations. In Figure 5 we plot with dotted magenta lines the curves corresponding to these limits. The curves are symmetric about  $180^\circ$  (in fact symmetry properties of sky motions hold more generally in the non-coplanar case; see section 2.1 of Jedicke (1996).

According to Figure 5, most of the 628 unknown objects agree with our model, in the sense that most are consistent with asteroids from the main belt. They are located at the bottom of the plot around  $\mu = 0.2 - 0.8''/\text{min}$  and between the two dotted curves corresponding to  $a_a = 2.0$

and  $a_a = 3.5$  AU. About 16 objects (2.5% of the total) marked with circles rise above the  $a = 1.3$  NEO limit and above the main vertical group at the respective elongation. We mark these objects with “fit” or “best” in the last column of Table 4, treating them as potential NEOs. One can clearly distinguish three major outliers showing the fastest proper motions, namely VBVI213 at  $\mu = 7.17''/\text{min}$  and VBTU222 at  $\mu = 2.12''/\text{min}$  observed at ESO/MPG, and VTU021 at  $\mu = 4.61''/\text{min}$  observed at the INT. We mark them with “best” in the last column of Table 4, treating them as our best NEO candidates.

The fastest object was recorded under the acronym VBVI213 and it moved about 10 times faster than all other MBAs observable close to opposition, so it represents our best NEO candidate. This object was clearly visible on 8 CCD images, leaving a 20 pixel trail owing to the relatively long 2 minute exposures. It moved in the opposite direction and about 10 times faster than all other asteroids visible in the same field. In Figure 6 we include the image of this field (CCD#5 of WFI), presenting the corresponding 8 frame animation in the online electronic version of the paper. The image is displayed in normal sky orientation and the field of view is about  $8' \times 16'$  (one WFI CCD), with pixel size  $0.714''$  (in  $3 \times 3$  binning). Four MBAs marked with circles are visible moving to the upper right, while the NEA candidate is visible as a trail in the bottom part (enlarged twice in the left corner inset). The exposure time was 2 minutes and the cadence between frames was 3.3 minutes.

Most of our fields were observed near opposition ( $150^\circ < \epsilon < 210^\circ$ ) and all agree well with our model. In Figure 5 there are about three fields located farther from opposition between  $130^\circ < \epsilon < 140^\circ$  for which most unknown objects do not match our model which does not hold due to our basic (circular and coplanar) orbital assumptions (proper motions in the model are close to zero, whereas the real orbits give a small but noticeable component to the proper motions).

Our second NEO search method uses the “NEO Rating” tool developed by the Minor Planet Center (MPC) which calculates a score for possible NEOs based on the expected proper motion of the MBA population distribution (MPC, 2011). Running this tool for all unknown ESO/MPG objects, we obtained NEO scores (“No-ID” probabilities) of 100% for three objects: VBTU197, VBTU222 and VBVI213 which confirm our findings using the first model. Running the NEO Rating for all unknown INT objects we confirm with 100% score two INT objects, VTU021 and VTD003, plus VITB01 with a relatively high score (77%). We plot with circles all these NEO candidates in Figure 5 and we include the scores in Table 4. All other objects from all runs received very low MPC rates (smaller than 5%), consistent with our MBA classification derived from our model.

Our third NEO search method uses the calculated MOID derived from the preliminary orbits derived with FIND\_ORB. The results are included in Table 4 and they mostly agree with the other two methods, showing in most cases the reliability of the derived preliminary orbits, especially for the objects observed closed to opposition.

Unfortunately most NEO candidates were observed in only one night and only one object was reobserved during a second night, namely VBTU203 = 2008 EN144. Two NEA candidates observed at INT were identified later with known objects, namely VTD003 = 2010 CJ33 and VIT005 = 2000 SN27. Based on their updated observed arcs, they are not NEAs, so we mark them by \* in Table 4. Dropping them from the list, we count in total 16 NEO candidates; this number should be considered an upper bound. Four objects have MPC scores of 100%, small MOIDs (less than 0.1 AU) and they agree mostly with our model, so they represent our best 4 NEO candidates: VBVI213, VBTU222, VBTU197 (observed at ESO/MPG) and VTU021 (observed at the INT). We write their acronyms in bold in the first column of Table 4. There was

no NEO candidate observed with Swope, checking all three methods.

We checked the remote possibility that some NEO candidates could be identified with Earth artificial satellites or space debris. In this sense, we checked all our observed fields against known Earth satellites by using the satellite identification server developed by Skvarc (2010b) based on the software SAT\_ID of Gray (2011b). No satellite with proper motion slower than  $0.25''/\text{min}$  (corresponding to geostationary orbits) was found within one degree of any observed fields. Known and unknown space debris could also be studied statistically, according to Schildknecht (2007). Compared with NEO candidates, space debris move at very fast speed with angular velocities ranging from a few arc seconds per second (i.e., a few arcminutes per minute, at least 10 times faster than our fastest NEO candidate) to more than 1,000 arcseconds per second with respect to the stellar background. Thus, we drop any possibility that any of our unknown objects could be associated with artificial satellites or space debris.

## 4. Discussion

### 4.1. Comparison with the known asteroid population

We compare the major orbital parameters of all unknown objects observed at ESO/MPG, Swope and INT with the entire known asteroid population at 10 Dec 2010 (541,260 orbits) based on the ASTORB database (Bowell, 2011).

In Figure 7 we plot two classic asteroid orbital distributions, namely  $e$  versus  $a$  (left) and  $i$  versus  $a$  (right). We overlay in colours all the unknown objects observed in our survey, including official discoveries, later identifications (based on MPC orbits) and outstanding objects (based on FIND\_ORB orbits). One can easily observe that the majority of our objects fit both orbital distributions very well, marking the four major Kirkwood gaps and a few known families. Only 105 points represent our official discoveries and later identifications, while 523 points represent outstanding objects (five times more). Because outstanding objects have orbits calculated with FIND\_ORB, at least statistically this confirms the ability of FIND\_ORB to calculate preliminary orbits based on very small arcs.

### 4.2. Comparison between facilities

In Figure 8 we plot the distribution of the observed apparent magnitude  $R$  (left panel) and the calculated absolute magnitude  $H$  versus semimajor axis  $a$  for all unknown asteroids observed with ESO/MPG, Swope and INT. The limiting magnitude of each system is evident by the levels in the  $R$  plot above which the regions become depleted of data. For each fixed limiting  $R$ , we expect a negative trend of  $H$  versus  $a$ , as seen in the right panel. We observed unknown MBAs up to  $a \sim 3.3$  AU, which is considered about half the outer main belt region (Yoshida & Nakamura, 2007). As expected, both 2m facilities sampled well the middle region ( $2.6 \leq a \leq 3.0$ ) and the first half of the outer region ( $3.0 \leq a \leq 3.3$ ), while well over half of unknown objects sampled with the Swope 1m are in the inner region of the main belt ( $2.0 \leq a \leq 2.6$ ). Moreover, according to Table 2, both ESO/MPG and INT discovered about the same number of MBAs as the number of known MBAs. Thus, a 2m survey could bring an important contribution to knowledge of the main belt, being expected to double the present number of known MBAs to more than one million.

According to the O–C plots for known MBAs (right panel of Figure 2, 3 and 4) and to the O–C standard deviation of  $0.15''$  for both NEA and known MBA datasets, ESO/MPG appears to have the best astrometry required for accurate follow-up, recovery and discovery across the

whole WFI camera. With standard deviations of  $0.18''$  for the known MBA dataset and  $0.39''$  for the NEAs, the Swope telescope represents an adequate 1m facility for asteroid studies at limiting magnitude  $R \sim 20.5$  mag. The field of the INT/WFC appears the most distorted, these O–C positions showing the widest spread in Figure 4 and a standard deviation about 4 times larger compared with the other two facilities. Although the INT astrometry is acceptable around the centre of WFC and could be used to follow-up known objects expected to appear close to the centre, the INT field should be corrected in order to reach more accurate astrometry across the entire WFC field.

Comparing the position of the centroid of the known bulk of MBAs with respect to the calculated positions, we conclude that the USNO-B1 catalog is less appropriate for astrometric reduction due to larger residuals, and we recommend instead UCAC-2 or UCAC-3 which appear to give more accurate results and therefore to be the current best representation of the Hipparcos frame up to magnitude 16. Nevertheless despite the superior accuracy from using the UCAC system, it still has shortcomings for the astrometry of fast moving objects such as the limited north declination coverage of UCAC-2 and the faulty northern proper motion system of UCAC-3.

#### 4.3. Distribution of the unknown MBA and NEO candidates

With the original 1m Spaceguard survey approaching its goal and limits, new 2m surveys such as Pan-STARRS will soon take over, increasing the detection limits in both size and depth in the Solar System. Based on our ESO/MPG and INT data, we briefly evaluate here the limits of such a 2m survey.

The left panel of Figure 9 plots the histogram showing the observed apparent magnitude  $R$  for all the unknown objects observed at ESO/MPG (red colour), Swope (green), the INT (blue) and the total (black dots). Apparently, the dark time at ESO was most efficient to detect unknown objects at  $R \sim 20.6$  mag, allowing a limit  $R \sim 21.5$  mag. This detection limit is consistent with the actual 1.8m Pan-STARRS 1 which is expected to reach  $R \sim 22$  mag (Grav, 2009). The INT reached maximum detection at  $R \sim 20.2$  mag and a more shallow cutoff at  $R \sim 21.2$  mag, about 0.3 mag less faint than ESO/MPG despite its larger aperture, probably due to the worse observing conditions at the INT. The 1m Swope reached a maximum detection at  $R \sim 19.8$  mag and a limiting magnitude at  $R \sim 20.4$  mag, about one magnitude lower than other 2m facilities. We include these limits in Table 2.

The right panel of Figure 9 plots the histogram showing the calculated absolute magnitude  $H$  for the unknown objects observed at the three facilities. Five objects fall outside the  $H$  range of the plot, namely the brightest object VB037 identified as the jovian Trojan 2001 TB234 ( $H = 13.3$ ) and the faintest four objects VBTO016 ( $H = 22.7$ ), VBTU222 ( $H = 24.7$ ), VBVI213 ( $H = 25.3$ ) and VTU021 ( $H = 26.4$ ). The last four are visible as clear individual points in Figure 8 (right) and the last three are among our best NEO candidates (Table 4). The  $H$  histograms are more evenly distributed, showing 2–3 maxima (possibly not all real) for each facility and an overall maximum at  $H \sim 17.4$  mag. This limit can be regarded as the limiting  $H$  giving completeness for a 2m class facility for the entire main belt (including the outer region). According to Yoshida & Nakamura (2007), this limit corresponds to S-class asteroids about 1km in diameter, thus virtually all S-type MBAs larger than this limit should be accessible to a 2m telescope (including ESO/MPG and INT) in good weather conditions.

As we saw in Figure 8 (left),  $R \sim 21.6$  mag represents the limiting apparent magnitude for the ESO/MPG. Most MBAs have absolute magnitudes between  $15 < H < 21$  mag, consistent with sizes between 170m and 6km, assuming albedos between 0.05 and 0.25 (NASA, 2011). The four best NEO candidates have the following  $H$  and sizes, assuming the same limits for their albedos:



VTU021:  $H = 26.4$  mag, 13–31 m; VBVI213:  $H = 25.3$  mag, 22–55 m; VBTU222:  $H = 24.7$  mag, 30–70 m; VBTU197:  $H = 18.9$  mag, 440–980 m.

In the left panel of Figure 10 we plot the calculated MOID versus the elongation  $\epsilon$  for the unknown objects observed at ESO/MPG (red), Swope (green) and INT (blue). With a dotted line we mark the MOID= 0.3 limit for NEAs below which all our NEO candidates appear. Based on this plot, there is no apparent favorable elongation to discover NEOs.

In the right panel of Figure 10 we plot the calculated MOID versus the observed ecliptic latitude  $\beta$  for the unknown objects observed at ESO/MPG (red), Swope (green) and INT (blue). Most unknown objects and NEO candidates were observed at low latitudes, under  $10^\circ$ . Most NEO candidates are observed at low latitudes and there is no particular favorable detection latitude with respect of the MBAs.

#### 4.4. Survey statistics for 2m and 1m facilities

Based on the statistics available from our ESO/MPG, Swope and INT surveys, we can evaluate the unknown MBA and NEA population observable at low latitudes ( $|\beta| < 10^\circ$ ) by 2m and 1m surveys. We include these results in Table 2.

##### 4.4.1. Unknown MBA density

Using data from our ESO/MPG survey (the best performing 2m facility) we observed in the  $10^\circ$  latitude range 347 known objects and 467 unknown objects scanning 13 square degrees. This gives an average of 27 known and 36 unknown MBAs per square degree visible to limiting magnitude  $R \sim 21.5$  mag in 2 min exposure time using the ESO/MPG. We include these findings at the end of Table 2. These numbers give for ESO/MPG a MBA ratio known:unknown = 0.7. We compare below our findings with other authors.

Counting data from our Swope survey we observed 35 unknown objects and 65 known objects within  $10^\circ$  latitude range from the ecliptic scanning about 5 square degrees of sky. This gives an average of 11 known objects and 7 unknown objects per square degree visible to limiting magnitude  $R \sim 20.4$  mag in 2 min exposure time with a 1m facility. The total number agrees with earlier results from the Spacewatch 0.9m which detected for the whole survey 16 asteroids per square degree.

Boattini et al. (2004) conducted a 3 night pilot search and follow-up program to detect NEAs using the ESO/MPG with WFI in  $3 \times 3$  binning mode (i.e., same facility and setup as us). During the last two nights, the authors scanned in good weather conditions a total of 24 square degrees, counting an average of 10 known and 12 unknown asteroids (mostly MBAs) per square degree. This gives a ratio known:unknown = 0.8 which is consistent with our findings. Nevertheless, both their numbers are about three times less than our findings. Their survey strategy was a bit different than ours, namely they observed at small solar elongation during the first and last part of the night and observing near opposition during the middle part. Also, for identification they used mostly automated software, although some data were reduced with Astrometrica. It is well known that the eye and brain are better than computer software in detection of moving objects by a factor of 3/2 based on experience of Spacewatch II (Boattini et al., 2004) or by 1 – 1.5 mag according to other authors (Yoshida et al, 2003). Both these factors could explain the lower density of asteroids (mostly MBAs) found by Boattini et al. (2004) compared with our statistics.

Wiegert et al (2007) searched 50 fields (50 square degrees) from the CFHT Legacy Survey (CFHTLS 3.6m) observed in  $r'$  close to opposition and within a  $2^\circ$  latitude range from the ecliptic. The moving objects were detected automatically by using the SExtractor software with a

threshold  $3\sigma$ . The authors found an average of 70 asteroids per square degree up to  $r' \sim 21.5$  mag (Wiegert, 2011), which agrees well with our findings.

Using the Subaru 8.3m telescope equipped with the large field SuprimeCam with 7 sec exposures Yoshida et al (2003) surveyed 3 square degrees near opposition and the ecliptic (SMBAS I survey) and found 92 asteroids per square degree to limiting magnitude  $R = 21.5$  mag. Using the same facility to image 4 square degrees using 2 second exposures (SMBAS II survey), Yoshida & Nakamura (2007) found an average of 75 objects per square degree to the same limit. In these surveys, moving objects were detected by human inspection. Our findings using the ESO/MPG are very close to their densities, taking into account our lower S/N due to Subaru's larger aperture and their pointing at lower latitudes.

Using one single 8.4m mirror of the Large Binocular Telescope (LBT), Ryan et al (2009) studied the asteroid distribution in the ecliptic, finding up to  $V = 22.3$  mag (close to  $R \sim 21.5$  mag our limit) a density of 85 asteroids per square degree. Asteroid detection was performed visually using a three-color method. Their density found is very close to ours, counting our total number of objects (63 objects per square degree).

#### 4.4.2. Unknown NEA density

Counting the NEO candidates from Table 4, ESO/MPG produced 8 NEO candidates and 3 best NEO candidates scanning a field of 13 square degrees. This gives between 0.2 and 0.6 NEO candidates per square degree observable with this facility. The value 0.6 is an upper limit because we could not confirm our objects which were observed only in one night.

Scanning 40 WFC fields (13 square degree) within  $15^\circ$  latitude in good weather at ESO/MPG, Boattini et al. (2004) discovered 3 NEA candidates (including 2 confirmed NEAs), which gives a density of 0.2 NEA candidates per square degree, matching our findings counting only the best candidates. Comparing their results with those from the 1.8m Spaceguard II survey, the authors conclude that on average one NEA per 10 square degrees could be discovered with ESO/MPG and the WFI. This is consistent with our findings if we count only one object, namely our best NEA candidate, VBVI213. Counting all our NEO candidates, our result is 6 times more optimistic than that of Boattini et al. (2004).

According to Table 4, INT produced 8 unknown objects and only one best NEA candidate scanning a field of 10 square degrees. This gives between 0.1 and 0.8 NEO candidates per square degree observable with INT (mostly in bad conditions). These densities are similar with those found by ESO/MPG and consistent with any other 2m survey.

## 5. Conclusions

We have analysed our observations taken with the ESO/MPG 2.2m in La Silla, the Swope 1m in Las Campanas and the INT 2.5m in La Palma. The total sky surveyed during 11 nights was about 29 square degrees, which allowed us to study statistics of MBAs and NEAs observable nowadays by other 1–2m facilities. Our main conclusions are:

- These telescopes are successful at following up faint objects soon after discovery, preventing their loss, recovering NEAs at their second or later opposition and eliminating NEA candidates and Virtual Impactors.
- The majority of our unknown objects are consistent with MBAs, based on two evaluation methods. Up to 16 unknown objects could represent NEO candidates from which 4 represent our best NEO candidates according to three evaluation methods.

- The O-C residuals for known MBAs and program NEAs amount to 0.15'' for the ESO/MPG, 0.39'' and 0.18'' for Swope and 0.42'' and 0.66'' for the INT, whose prime focus field is the most distorted (especially the three non-central CCDs) and needs to be corrected in order to improve the astrometry.
- The UCAC-2 catalog is better than USNO-B1 which shows an offset of 0.1'' to the North, consistent with previous findings of other authors.
- Published orbits (specifically  $a$ ,  $e$  and  $i$ ) of known asteroids are very similar to our calculated orbits using the FIND\_ORB software based on our observed very small arcs.
- Based on statistics derived from our data, we could assess the observability of the unknown MBA and NEA populations using 1m and 2m class surveys. Employing a 1m facility one can observe today fewer unknown objects than known MBAs and virtually no new NEO. Using a 2m facility, a slightly larger number of unknown than known MBAs could be detected (up to about  $a = 3.2$  AU), consistent with objects having sizes between 170m and 6km (taking into account the limits of the main belt and the albedo range). Between 0.1 and 0.8 new NEO candidates per square degree could be discovered using a 2m telescope.
- A basic model assuming circular and coplanar orbits of the asteroids and Earth could be used in order to check any large all sky survey for potential NEO candidates. Employing the proper motion and Solar elongations, this model does not depend on calculated quantities such as orbital elements possibly subject to errors. Compared with other tools such as the MPC's NEO Rating and the calculated preliminary orbits, this model seems very accurate at small elongations ( $\pm 30^\circ$  from opposition) but, based on the residuals in our data, smaller elongations (around  $120 - 140^\circ$ ) need further study.

## 6. Acknowledgements

This work was based on observations made with the ESO/MPG telescope at La Silla Observatory under programme ID 080.C-2003(A), the Swope telescope at Las Campanas Observatory (CNTAC 2008), both granted under Chilean time, and the INT telescope in La Palma under Director's Discretionary Time of Spain's Instituto de Astrofísica de Canarias (CAT DDT 2010). OV acknowledges ESO, LCO and IA/UCN for supporting the runs in Chile for himself and the students, and also to the ING, IAC and the IAA for supporting the run in La Palma for the students. OV and JL gratefully acknowledge support from the spanish "Ministerio de Ciencia e Innovación" (MICINN) project AYA2008-06202-C03-02. This research has made intensive use of the Astrometrica software developed by Herbert Raab, very simple to install and use by students and amateur astronomers. We also used the image viewer SAOImage DS9, developed by Smithsonian Astrophysical Observatory and also IRAF, distributed by the National Optical Astronomy Observatories, operated by the Association of Universities for Research in Astronomy, Inc. under cooperative agreement with the National Science Foundation. Special thanks are due to Bill Gray for providing FIND\_ORB and installation assistance. OV also acknowledges to Paul Wiegert for feedback necessary to compare MBA data observable with CFHT and the ESO/MPG telescopes. Thanks are due to Fumi Yoshida and Tsuko Nakamura for sharing their SMBAS data and interest. We also acknowledge to Jure Skvarc for his satellite identification software and to Lilian Dominguez for providing some references about space debris. Thanks are also due to Alain Maury who helped us to count NEA discoveries made in Europe. Acknowledgements are due to the referee whose constructive suggestions helped us to improve the paper.

## References

- Assafin, M., et al., 2010, *Astronomy & Astrophysics* 515, A32
- AstDyS, 2011, *Asteroids Dynamic Site*, <http://hamilton.dm.unipi.it/astdys/>
- Benecchi, S.; Sheppard, S. S.; Vaduvescu, O.; Pozo, F.; Barr, A.; Tudorica, A.; Sonka, A., 2008, MPC 64096, 9
- Benecchi, S.; Sheppard, S. S.; Vaduvescu, O.; et al., 2009, MPC 64484, 5
- Benecchi, S.; Sheppard, S. S.; Vaduvescu, O.; et al., 2009, MPC 64753, 3
- Benecchi, S.; Sheppard, S. S.; Vaduvescu, O.; et al., 2009, MPC 66688, 10
- Benner, L., 2010 - private communication
- Birlan, M., et al, 2010, *Astronomy & Astrophysics*, 511, A40
- Boattini, A., et al., 2003, *Earth, Moon and Planets*, 93, 239
- Boattini, A., et al., 2004, *Astronomy & Astrophysics*, 418, 743
- Bowell, E. and Muinonen, K., 1994, in *Hazards due to Comets and Asteroids*, 149
- Bowell, E., 2011, ASTORB database, <ftp://ftp.lowell.edu/pub/elgb/astorb.html>
- Cavadore, C.; Vaduvescu, O.; Birlan, M.; Tudorica, A.; Toma, R.; Sonka, A.; Oprisceanu, C.; Vidican, D. et al., 2008, MPC 63369, 9
- Chapman, C. R., & Morrison, D., 1994, *Nature*, 367, 33
- EARN, 2011 - *Near Earth Asteroids Data-Base*, <http://earn.dlr.de/nea/>
- Elst, E. W.; Masi, G.; Lagerkvist, C.-I.; Boattini, A.; Behrend, R.; Vaduvescu, O., 2008, MPC 63591, 10
- Elst, E. W.; Lagerkvist, C.-I.; Boattini, A.; Vaduvescu, O.; Greco, C.; Behrend, R., 2008, MPC 63129, 5
- Elst, E. W.; Lagerkvist, C.-I.; Boattini, A.; Boehnhardt, H.; Vaduvescu, O., 2008, MPC 62871, 8
- Elst, E. W.; Vaduvescu, O.; Birlan, M.; Tudorica, A.; Toma, R.; Sonka, A.; Oprisceanu, C.; Vancea, C.; Vidican, D., 2008, MPC 62573, 3
- Elst, E. W.; Lagerkvist, C.-I.; Boattini, A.; Vaduvescu, O., 2009, MPC 66195, 4
- Elst, E. W.; Lagerkvist, C.-I.; Boattini, A.; Vaduvescu, O., 2009, MPC 65331, 2
- Elst, E. W.; Masi, G.; Lagerkvist, C.-I.; Boattini, A.; Behrend, R.; Vaduvescu, O., 2009, MPC 65045, 7
- EURONEAR, 2011 - *Observing Tools - Planning NEA observations*, <http://euronear.imcce.fr/tiki-index.php?page=Planning>
- Fitzsimmons, A., Vaduvescu, O. & Asher, D., 2009, MPC 66457, 4
- Fitzsimmons, A., Vaduvescu, O., Tudorica, A. & Badea, M., 2009, MPC 65927, 9
- Fitzsimmons, A., Vaduvescu, O. & Tudorica, A., 2009, MPC 65332, 1
- Grav, T., 2009 - communication on the MPML discussion list
- Gray, B., 2011a - FIND\_ORB, [http://www.projectpluto.com/find\\_orb.htm](http://www.projectpluto.com/find_orb.htm)
- Gray, B., 2011b - SAT\_ID software, [http://www.projectpluto.com/sat\\_id.htm](http://www.projectpluto.com/sat_id.htm)
- Holman, M., Fitzsimmons, A., Grav, T., Vaduvescu, O., 2009, MPC 66196, 2
- Holvorcem, P. R., Schwartz, M., Vaduvescu, O., Tudorica, A., Dumitru, D., 2010, MPEC 2010-E39
- IMCCE, 2011 - *Ephemerides*, <http://www.imcce.fr/en/ephemerides/>
- Jedicke, R., 1996, *Astronomical Journal*, 111, 970
- Kern, S. D.; Sheppard, S. S.; Vaduvescu, O.; Schechter, P. L., 2008, MPC 63365, 10
- Kern, S. D.; Sheppard, S. S.; Vaduvescu, O.; Schechter, P. L., 2009, MPC 66190, 11
- Kolena, J., 1999 - *Conversion of Asteroid Proper Motion to Distance from the Sun*, <http://www.phy.duke.edu/~kolena/asteroid.html>
- Milani, A. and Gronchi, G. F., 2009, *Theory of Orbit Determination*
- Minor Planet Center (MPC), 2011, <http://minorplanetcenter.net/>
- Morbidelli A. et al., 2002, in *Asteroids III*, 409
- Morbidelli A., 2005, *Asteroid Population Models*, in *Dynamics of Population of Planetary Systems*, Proc. IAU Colloq. 197, 229
- NEODyS, 2011, *Near Earth Objects - Dynamic Site*, <http://newton.dm.unipi.it/neodyS/>
- NASA & JPL, 2011, *Near Earth Object Program*, <http://neo.jpl.nasa.gov/>
- O'Brien, D. P. & Greenberg, R., 2005, *Icarus*, 178, 179
- Pozo, F.; Barr, A.; Vaduvescu, O. et al., MPEC, 2008-U48
- Raab, H., 2011, *Astrometrica software*, <http://www.astrometrica.at>
- Ryan E. R., et al., 2009, *The Astronomical Journal*, 137, 5134
- Smithsonian Astrophysical Observatory, 2011, *SAOImage DS9*, <http://hea-www.harvard.edu/RD/ds9/>
- Schildknecht, T., 2007, *Optical surveys for space debris*, *Astron Astrophys Rev*, 14, 41-111
- Scotti, J. V.; Pozo, F.; Barr, A.; Vaduvescu, O. et al., 2008, MPEC, 2008-U45
- Scotti, J. V.; Pozo, F.; Barr, A.; Vaduvescu, O. et al., 2008, MPEC, 2008-U46
- Sheppard, S. S.; Vaduvescu, O.; Galad, A.; Tudorica, A.; Nedelcu, A.; Toma, R.; Oprisceanu, C., 2008, MPC 62258, 1
- Skvarc, J., 2010a, *Asteroid Residual Calculator* <http://www.fitsblink.net/residuals/>
- Skvarc, J., 2010b, *Identification of satellites from astrometric positions* <http://www.fitsblink.net/satellites/>

Spaceguard Foundation, 2011, <http://spaceguard.esa.int>  
 Tholen, D. L., Bernardi, F., & Micheli, M., 2008, AAS DPS Meeting 40, 434  
 Tholen, D. J.; Vaduvescu, O.; Birlan, M.; Tudorica, A.; Toma, R.; Nedelcu, A.; Sonka, A.; Opriseanu, C. et al., 2008  
 MPC 62262, 5  
 Tholen, D. J.; Elst, E. W.; Lagerkvist, C.-I.; Boattini, A.; Behrend, R.; Vaduvescu, O., 2009, MPC 65636, 2  
 Tubbiolo, A. F.; Vaduvescu, O.; Tudorica, A.; et al., 2008, MPEC, 2008-K66  
 Vaduvescu, O. & Tudorica, A., 2008, MPC 63125, 6  
 Vaduvescu, O., 2009, *How we discovered between 56 and 483 asteroids in 3 nights*, Vega 129, iul 2009 (electronic  
 magazine), Bucharest Astroclub (in Romanian) <http://www.astroclubul.ro/index.php/revista-vega/arhiva-vega>  
 Wiegert, P. et al, 2007, Astronomical Journal, 133, 1609  
 Wiegert, P., 2011 - private communication  
 Yoshida, F. et al, 2003, Publ. Astron. Soc. Japan, 55, 701  
 Yoshida, F. & Nakamura, T., 2007, Planetary and Space Science, 55, 1113  
 Young, J.; Vaduvescu, O.; Tudorica, A., et al., 2008, MPEC, 2008-K63

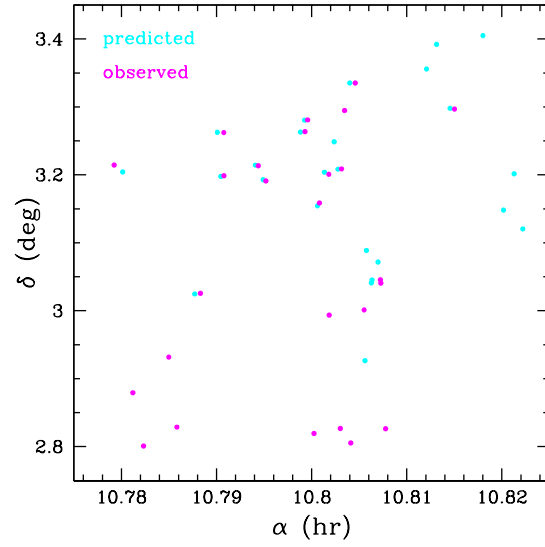


Figure 1: Pairing the unknown objects observed in multiple nights based on positions derived from the extrapolated arc. Cyan points stand for extrapolated positions of objects observed in the first night and magenta points mark objects observed in the second night in the follow-up field.

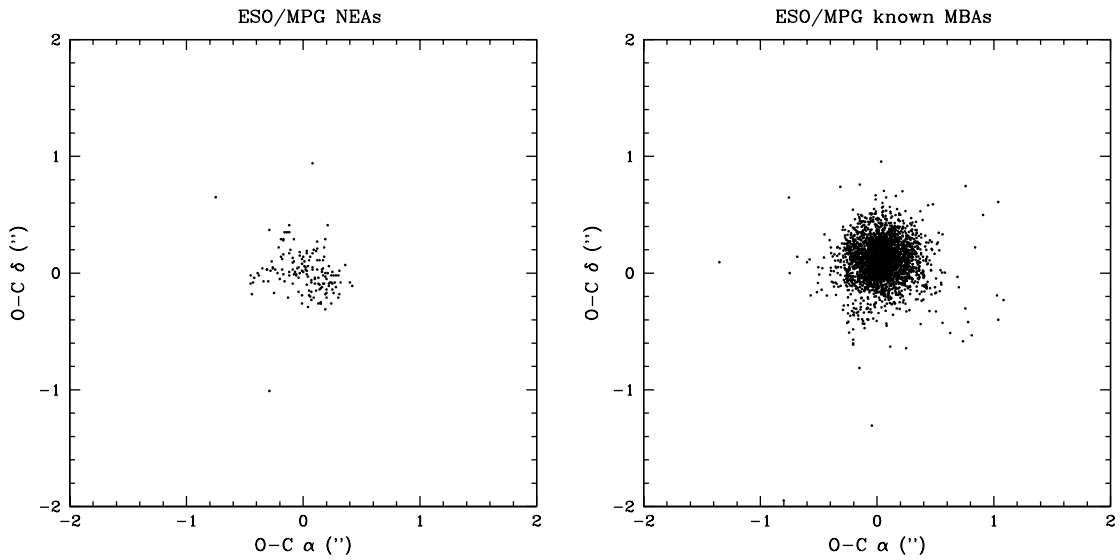


Figure 2: O-C (observed minus calculated) residuals for program NEAs and known MBAs observed at ESO/MPG.

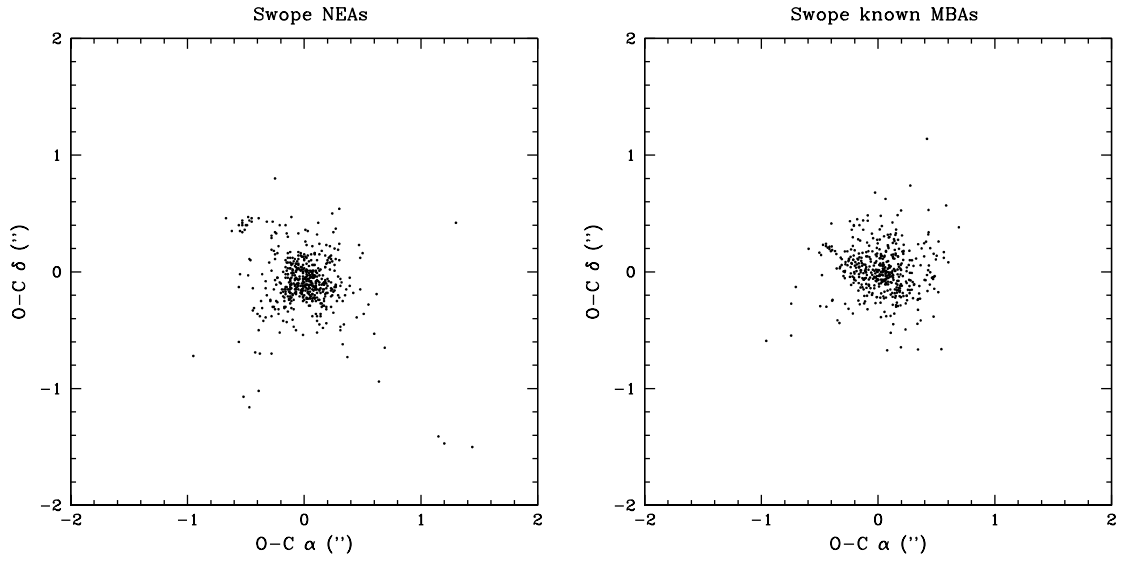


Figure 3: O-C (observed minus calculated) residuals for program NEAs and known MBAs observed with Swope telescope.

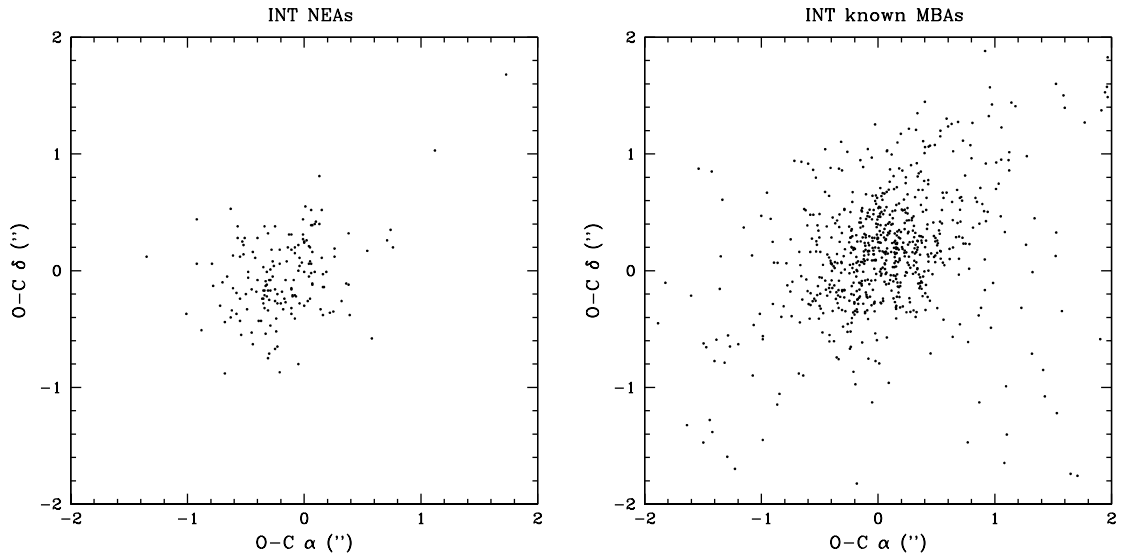


Figure 4: O-C (observed minus calculated) residuals for program NEAs and known MBAs observed with the INT.

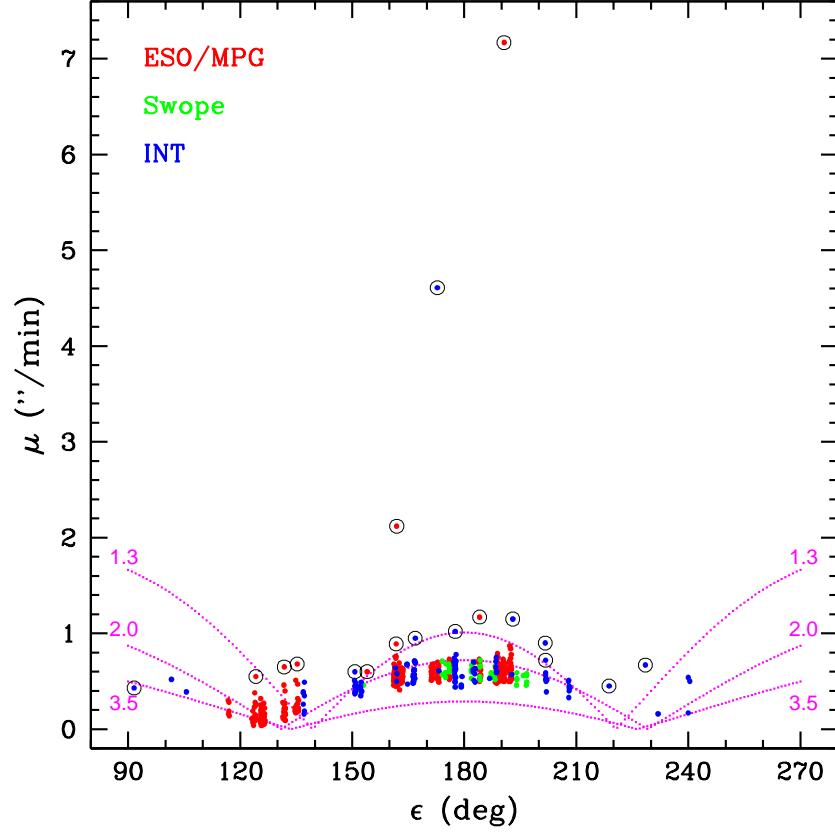


Figure 5: Basic orbital model using the asteroid observed proper motion  $\mu$  and the Solar elongation  $\epsilon$ . We plot all unknown objects observed at ESO/MPG (red), Swope (green) and INT (blue). The three overlaid dotted magenta curves correspond to asteroids orbiting between  $a = 2.0$  and  $a = 3.5$  AU (Main Belt) and  $a = 1.3$  (Near Earth Objects limit). The model allows us to easily flag NEO candidates in a survey. We mark with circles our NEO candidates and we include their properties in Table 4.



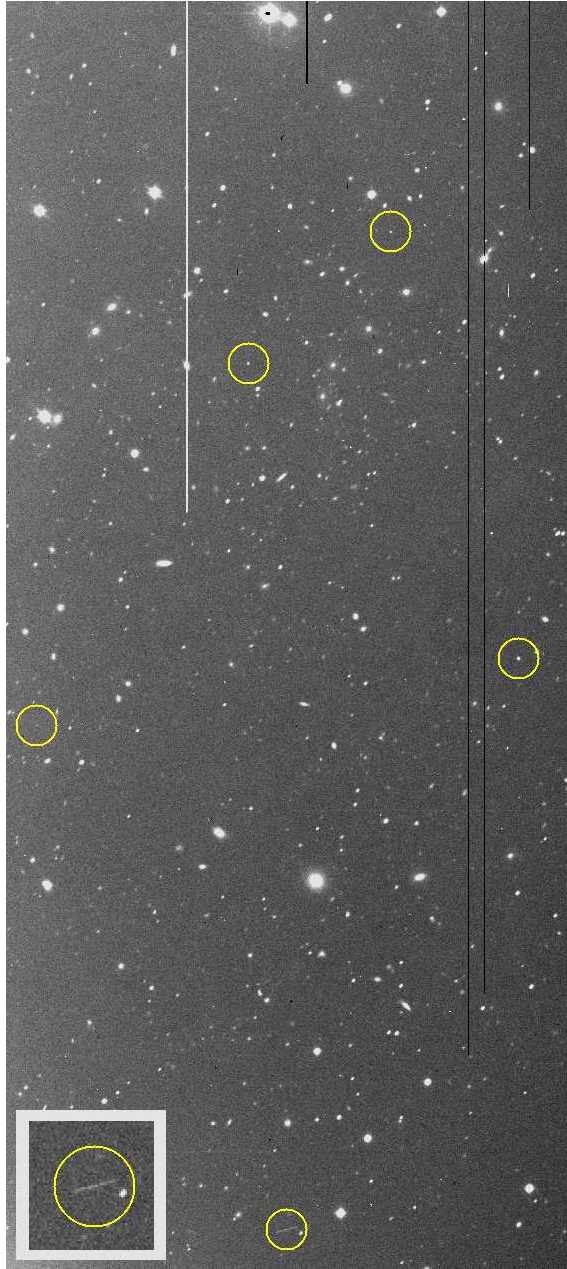


Figure 6: VBVI213, our best NEO candidate, at the bottom of the  $8' \times 16'$  ESO/MPG WFI CCD#5, moving in the opposite direction to the four MBAs marked above, and about 10 times faster. The image is displayed in normal sky orientation (N up, E left) and the inset zooms in on the NEO candidate. An animation including all 8 available frames is available online.

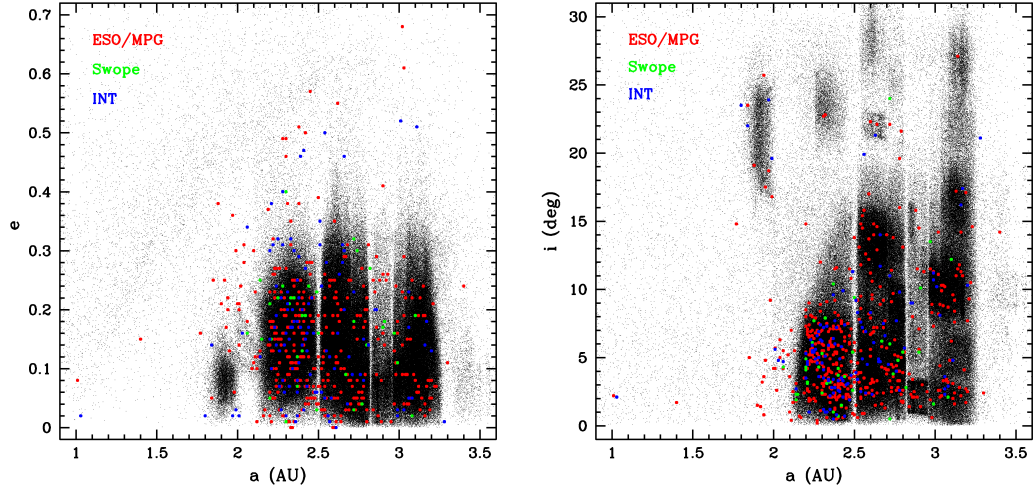


Figure 7: Orbital distributions of 628 unknown objects observed at ESO/MPG (red points), Swope (green) and INT (blue) compared with the entire known asteroid population (ASTORB - 541,260 fine black points). Although our preliminary orbits were derived using mostly short arcs, the distributions are consistent with the known MBA population, showing the usefulness of the FIND\_ORB orbital fit in  $a$ ,  $e$  and  $i$ .

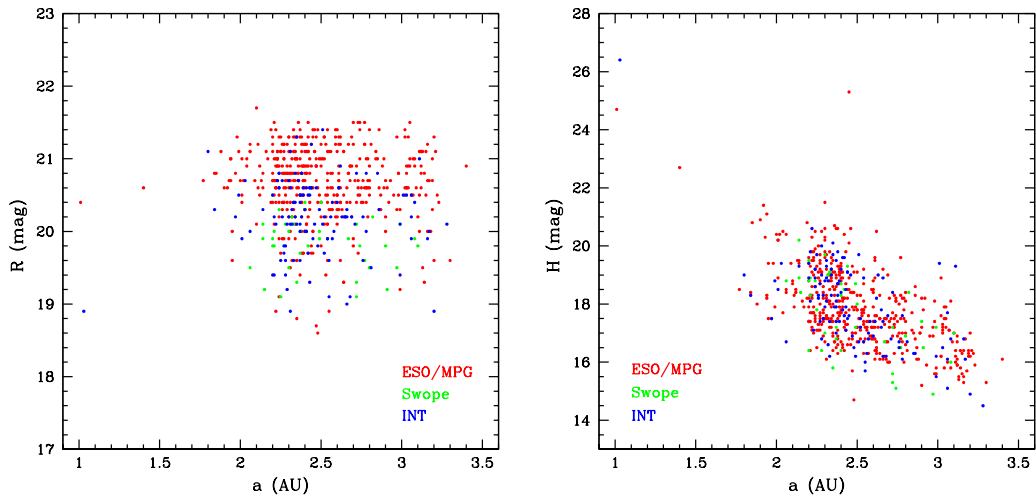


Figure 8: The observed apparent  $R$  magnitude (left) and calculated absolute magnitude  $H$  (right) versus the semimajor axis  $a$  for the ESO/MPG unknown asteroids dataset (red points), Swope (green) and INT (blue). The three objects having the faintest  $H$  are among the best NEO candidates.

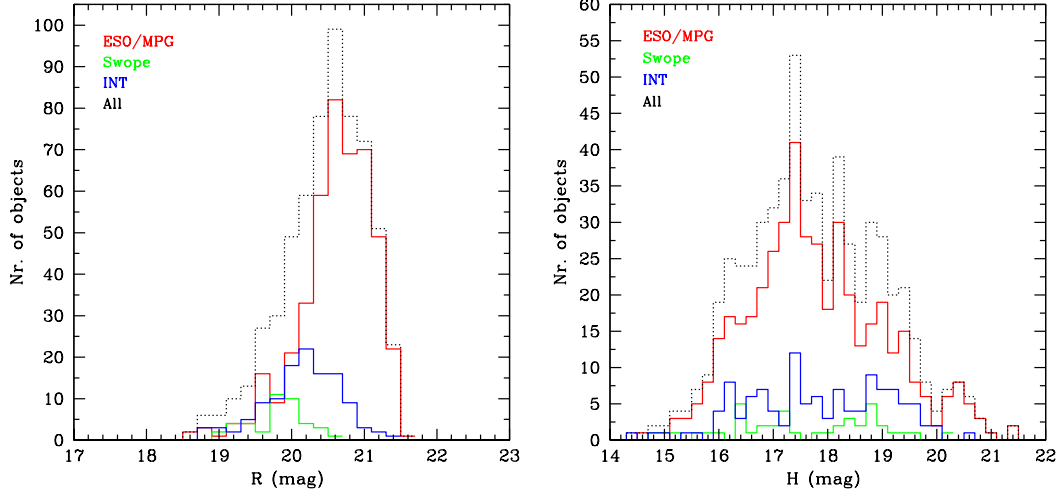


Figure 9: Histograms showing number of unknown objects as function of observed apparent  $R$  magnitude (left) and calculated absolute magnitude  $H$  (right) for the ESO/MPG dataset (red), Swope (green), INT (blue) and the total number of objects (black dots).

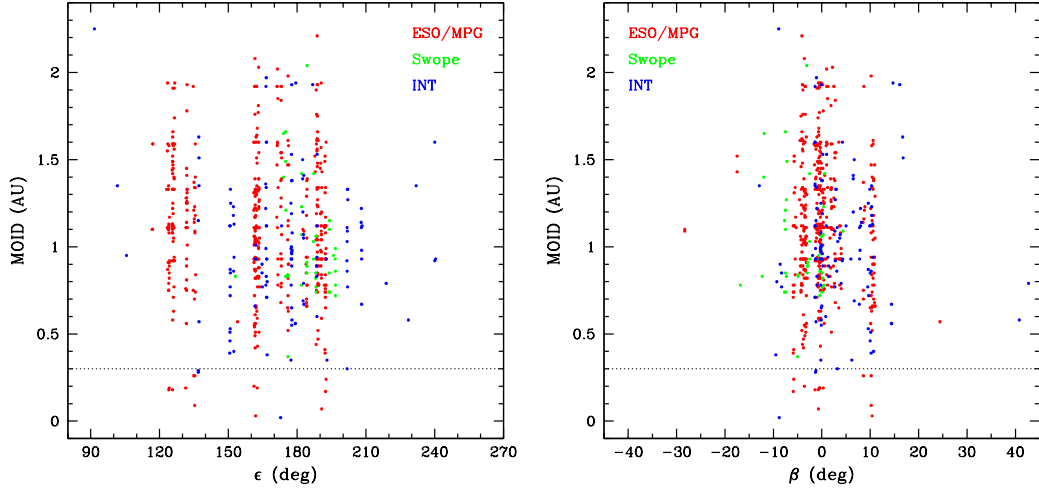


Figure 10: Minimal Orbital Intersection Distance (MOID) versus Solar elongation  $\epsilon$  (left panel), and versus ecliptic latitude  $\beta$  (right panel) for the unknown objects observed at ESO/MPG (red), Swope (green) and INT (blue). The dotted line at  $MOID < 0.3$  marks the NEO region under which all our NEO candidates appear.

Table 1: The observing log for NEA observations at INT. We list the name of the asteroid, its classification at time of observation, date of observation, expected apparent magnitude  $V$ , exposure time (seconds), number of observed positions, apparent motion  $\mu$  ( $''/\text{min}$ ), ephemeris uncertainty (arcsec) and observed orbital arc since discovery (d-days, m-months, y-years). Objects marked with \* represent special cases discussed in the paper.

Asteroid	Class	Date (UT)	$V$ (mag)	Exp (s)	Nr pos	$\mu$ ( $''/\text{min}$ )	$3\sigma$ ( $''$ )	Obs arc
2009 CW1	NEA	2009 Feb 12	19.9	20	10	3	40	9d
2009 CB2*	?	2009 Feb 12	20.1	60	5	3	1000	6d
2009 CA2	NEA	2009 Feb 12	20.0	30	8	1	30	9d
2003 SJ84*	NEA	2009 Feb 12	21.4	120	5	2	81	6y
2009 FF	PHA	2009 Apr 15	20.8	60	5	2	38	1m
2009 DZ	PHA	2009 Apr 15	21.1	120	6	1	3	1m
2009 FJ30	NEA	2009 Apr 15	17.8	30	5	5	9	18d
2009 FT	NEA	2009 Apr 15	19.2	30	6	4	1	18d
2009 FJ44	PHA	2009 Apr 15	19.5	60	5	1	2	16d
2009 FG19	PHA	2009 Apr 15	20.5	90	5	2	24	25d
2009 FH44	NEA	2009 Apr 15	19.8	60	5	2	1	16d
2009 FY4	PHA	2009 Apr 15	21.0	120	10	1	12	26d
2009 FV4	NEA	2009 Apr 15	21.1	90	5	1	26	26d
2009 FR30	NEA	2009 Apr 15	21.2	120	4	1	56	20d
2009 FT32	NEA	2009 Apr 15	20.8	30	5	11	42	24d
2009 VR25*	VI	2009 Nov 13	20.7	30	4	5	1400	2d
2009 VN1	NEA	2009 Nov 14	21.0	30	5	7	932	5d
2009 VQ	NEA	2009 Nov 14	20.9	30	5	7	3	6d
2009 KK	PHA	2009 Nov 14	21.2	60	5	2	270	6m
2010 DJ1*	NEA	2010 Feb 20	19.3	30	5	10	190	3d
2010 CF55	NEA	2010 Feb 20	20.8	90	3	3	39	5d
2010 CF12*	NEA	2010 Feb 20	19.8	90	2	10	?	8d
2010 DX1	NEA	2010 Feb 23	17.9	30	5	8	24	4d
2010 DF1	PHA	2010 Feb 23	20.5	60	4	3	94	6d
2007 RM133*	NEA	2010 Feb 23	21.4	120	5	1	490	3y
2000 SV20*	NEA	2010 Feb 25	21.0	120	4	1	2900	10y
2010 DC*	NEA	2010 Mar 03	20.1	120	8	1	58	17d
2009 FY4	PHA	2010 Mar 03	16.8	10	5	12	1	1y
2007 EF*	PHA	2010 Mar 03	18.2	10	8	20	1	3y
2000 CO101	PHA	2010 Mar 03	16.3	20	6	6	1	10y
2008 EE	NEA	2010 Mar 03	16.5	20	7	6	1	2y
2006 SS134	PHA	2010 Mar 03	20.5	20	3	12	2	4y
2010 DJ56	PHA	2010 Mar 03	20.9	180	4	2	3	11d
2007 JZ20	NEA	2010 Mar 03	20.8	180	5	1	1	3y
2008 TZ3	PHA	2010 Mar 03	21.1	120	7	2	1	2y

Table 2: Summary of the ESO/MPG, Swope and the INT runs.

Observations	ESO/MPG	Swope	INT	Total
Program NEAs	15	50	35	100
Nr of positions	156	506	169	831
O–C standard deviation (″)	0.15	0.39	0.42	—
Known MBAs	347	68	143	558
Nr of positions	2,976	680	733	4,389
O–C standard deviation (″)	0.15	0.18	0.66	—
Unknown objects	467	41	120	628
Nr of positions	4,183	261	574	5,019
Official discoveries	58	0	0	58
Later identifications	17	8	22	47
Outstanding objects	392	33	98	523
Nr. of nights	3	5	3	11
Nr. of observed fields	42	50	35	127
Sky coverage (square degrees)	13	6	10	29
Limiting magnitude ( $R$ )	21.5	20.4	21.2	—
Total nr. of objects	829	159	298	1,286
Total nr. of positions	7,315	1,447	1,476	10,239
Known MBAs density (obj/sq.deg)	27	11	14	—
Unknown MBAs density	36	7	12	—
Unknown NEOs density	0.2-0.6	0	0.1-0.8	—

Table 3: Minor Planet Circulars (MPC) and Minor Planet Electronic Circulars (MPEC) publishing our NEA observations

Telescope	MP(E)C	Reference
Swope	MPC 64484, 5	Benecchi et al (2008a)
Swope	MPC 64096, 9	Benecchi et al (2008b)
Swope	MPC 66688, 10	Benecchi et al (2009a)
Swope	MPC 64753, 3	Benecchi et al (2009b)
Swope	MPC 63365, 10	Kern et al (2008)
Swope	MPC 66190, 11	Kern et al (2009)
Swope	MPEC 2008-U48	Pozo et al (2008)
Swope	MPEC 2008-U46	Scotti et al (2008a)
Swope	MPEC 2008-U45	Scotti et al (2008b)
Swope	MPEC 2008-K66	Tubbiolo et al (2008)
Swope	MPC 63125, 6	Vaduvescu & Tudorica (2008)
Swope	MPEC 2008-K63	Young et al (2009)
ESO/MPG	MPC 63369, 9	Cavadore et al (2009)
ESO/MPG	MPC 63591, 10	Elst et al (2008a)
ESO/MPG	MPC 63129, 5	Elst et al (2008b)
ESO/MPG	MPC 62871, 8	Elst et al (2008c)
ESO/MPG	MPC 62573, 3	Elst et al (2008d)
ESO/MPG	MPC 66195, 4	Elst et al (2009a)
ESO/MPG	MPC 65331, 2	Elst et al (2009b)
ESO/MPG	MPC 65045, 7	Elst et al (2009c)
ESO/MPG	MPC 62258, 1	Sheppard et al (2008)
ESO/MPG	MPC 62262, 5	Tholen et al (2008)
ESO/MPG	MPC 65636, 2	Tholen et al (2009)
INT	MPC 66196, 2	Holman et al (2009)
INT	MPEC 2010-E39	Holvorcem et al (2010)
INT	MPC 66457, 4	Fitzsimmons et al. (2009a)
INT	MPC 65927, 9	Fitzsimmons et al. (2009b)
INT	MPC 65332, 1	Fitzsimmons et al. (2009c)

Table 4: Near Earth Object (NEO) candidates – fast unknown objects observed at ESO/MPG (first group) and the INT (second group). We list in bold 4 objects which qualify as the best NEO candidates, having small MOIDs, 100% NEO Rating score and fitting best the  $\epsilon - \mu$  model. The two one-nighter objects marked with \* are not NEAs according to their later identifications.

Acronym	$\mu$ ("'/min)	$\epsilon$ (°)	$R$	MOID (AU)	$a$ (AU)	$e$	$i$ (°)	Nr pos	$\sigma$ ("')	MPC score	Model
VB011	0.55	125	20.8	0.19	2.28	0.49	6.7	8	0.13	14	close
VB0203	0.65	132	20.8	0.75	1.84	0.05	23.5	16	0.26	10	fit
<b>VB0197</b>	0.68	135	21.4	<b>0.09</b>	3.02	0.68	8.2	7	0.38	<b>100</b>	<b>best</b>
VB0A002	0.60	154	19.8	0.57	2.50	0.39	13.8	3	0.08	22	fit
<b>VB0222</b>	<b>2.12</b>	162	20.4	<b>0.03</b>	1.01	0.08	2.2	5	0.16	<b>100</b>	<b>best</b>
VB0226	0.89	162	21.0	0.56	1.94	0.20	25.7	5	0.52	21	fit
VB0072	1.17	184	20.0	0.70	1.95	0.13	17.5	8	0.12	24	fit
<b>VB0213</b>	<b>7.17</b>	191	~20	<b>0.07</b>	2.46	0.57	2.0	7	0.31	<b>100</b>	<b>best</b>
VITB01	0.43	92	20.1	2.25	3.28	0.01	21.1	5	0.26	<b>77</b>	bad
VTD069	0.60	151	20.5	0.51	3.01	0.52	10.2	4	0.51	6	fit
VIT005 *	0.95	167	19.0	0.38	2.66	0.20	14.0	4	0.38	28	fit
VTD010	1.02	177	20.2	0.97	2.63	0.26	21.3	5	0.30	5	fit
<b>VTU021</b>	<b>4.61</b>	173	18.9	<b>0.02</b>	1.03	0.02	2.1	3	0.43	<b>100</b>	<b>best</b>
VTD003 *	1.15	193	19.3	0.35	2.43	0.14	3.3	4	0.35	<b>100</b>	fit
VTU031	0.90	202	20.5	0.92	1.99	0.03	19.6	5	0.14	10	fit
VTU028	0.72	202	20.6	0.30	2.39	0.46	7.2	3	0.26	15	fit
VBA003	0.45	219	21.1	0.79	1.80	0.02	23.5	5	0.08	18	fit
VTU020	0.67	228	20.3	0.58	1.84	0.14	22.0	6	0.31	25	fit